Titan Atmospheric Entry Radiative Heating

A. M. Brandis*† and B. A. Cruden‡
AMA at NASA Ames, Mountain View, CA, 94035, USA,

Detailed spectrally and spatially resolved radiance has been measured in the Electric Arc Shock Tube at NASA Ames Research Center for conditions relevant to Titan entry, varying atmospheric composition, free-stream density (equivalent to altitude) and shock velocity. Permutations in atmospheric composition include 1.1%, 2%, 5% and 8.6% CH_4 by mole with a balance of N_2 and 1.5% CH_4 / 0.5% Ar / 98% N_2 by mole, which is consistent with the current understanding of Titan's atmosphere. The effect of gas impurities identified in previous shock tube studies was also examined by testing in pure N_2 and deliberate addition of air to the CH_4/N_2 mixtures. The test campaign reported in this work, known as Test 61, measured radiation at velocities from 4.7 km/s to 8 km/s and free-stream pressures of 0.1, 0.28 and 0.47 Torr. These conditions cover a range of potential trajectories for flight missions, including a direct ballistic trajectory, a gravity assist fly-by, aerocapture or an extremely high-speed entry. Radiances measured in this work are substantially larger compared to that reported both in past EAST test campaigns and in other shock tube facilities. Depending on the metric used for comparison, the discrepancy can be as high as an order of magnitude. Due to the difference with previously reported data, a substantial effort was undertaken to provide confidence in the new results. With increased confidence in Test 61 and improved agreement with simulations, potential causes for erroneous results in previously reported data, such as the effect of oxygen due to air leakage, gas composition and purity, are discussed. The present work provides a new benchmark set of data to replace those published in previous studies. The results from Test 61 are available at https://data.nasa.gov/ [a].

I. Introduction

For certain planetary entry conditions, radiative heating from the bow shock over the vehicle may contribute sufficient heat load as to influence heat shield design. Codes for predicting radiative heating carry significant margin/uncertainty and require validation at conditions relevant to entry. One of the best ways to obtain validation data is through testing in shock tubes. The Entry Systems Modeling (ESM) project in NASA's Space Technology Mission Directorate is advancing the state-of-the-art in aerothermal modeling, by refining models for radiation and shock layer kinetics. The non-equilibrium radiation from the CN molecule is of particular interest to radiative heating during Titan entry. Two previous test campaigns (Tests 43 and 45 conducted from 2003 to 2005[1]) in the Electric Arc Shock Tube (EAST) and two test campaigns in the X2 shock tube[2,3] reported results inconsistent with simulations. Furthermore, Test 43 has been shown to be inconsistent with Test 45 and X2 data.[2] It was reported that the suspect results (EAST Test 43) were potentially due to issues with the radiance calibration and carbon contamination.[2,4] Even though these results have been shown to be potentially questionable, they are still frequently used as benchmark data for development of simulation models for Titan entry.[5–7] Since test campaigns 43 and 45, the EAST facility has undergone substantial upgrades, improving both the data quality and the quantity obtained. With updates to calibration techniques, and improved cleaning of the shock tube reducing carbon contamination,[4] it is warranted to conduct tests to update the previously reported experiments. Due to the limited data available prior to the present campaign and the poor level of agreement between previously reported data with

*Senior Research Scientist, Aerothermodynamics Branch, and Senior Member AIAA.
†Contact: aaron.m.brandis@nasa.gov
‡Senior Research Scientist, Aerothermodynamics Branch, and Associate Fellow AIAA
[a]Download EAST data at https://data.nasa.gov/docs/datasets/aerothermodynamics/EAST/index.html

either Boltzmann, standard QSS approaches or Collisional-Radiative (CR) models,[1,8,9] developing a model to accurately simulate non-equilibrium CN radiation has proven to be difficult.

II. Description of the EAST Facility

The EAST facility at NASA Ames Research Center was developed to simulate high-enthalpy, real-gas phenomena encountered by hypersonic vehicles entering planetary atmospheres. In recent years, the EAST facility at NASA Ames has been employed for the purpose of obtaining validation data for radiative heating. The shock tube produces high velocity flows in gases of known composition and densities relevant to various atmospheric entries. These flows are achieved by creating a sudden pressure discontinuity in the form of a normal shock wave that moves hypersonically into the gas in front of it. Because of the short time scales involved, the discontinuity does not have time to mix, but rather compresses the gas as it moves forward, much like a spacecraft will do to the atmosphere during planetary entry. This shock wave in the driven gas of EAST is therefore assumed to be analogous to the bow shock in an entry scenario. The radiating shock wave can be imaged as it passes through the shock tube, and separated into different wavelength ranges via spectroscopy. The spectroscopic imaging of the shock is important as the radiation varies significantly with wavelength. The ability to predict and model both the non-equilibrium and equilibrium radiance is dependent upon knowing the spectral features. Having confidence in spectral predictions is important for accurate simulations of radiative heating for an atmospheric entry vehicle.

EAST has the capability of producing super-orbital shock speeds using an electric arc driver with a driven tube diameter of 10.16 cm.[4,10] The region of valid test gas is located between the shock front and the contact surface that separates the driver and driven gases. The test duration is defined as the axial distance between these two points divided by the local shock velocity. The characteristics of the EAST arc driver result in test durations of approximately 4 - 10 μs. Though short, this test duration is often sufficient to capture the peak non-equilibrium shock radiation and the decay toward equilibrium conditions. When the shocked gas arrives at the location of the test section, spectrometers attached to Charge Coupled Devices (CCDs) are gated, and the spectral and spatial emission of the gas is analyzed. EAST utilizes four spectrometers per shot, each associated with four different wavelength ranges. These cameras are referred to as: VUV ($\sim$120 – 420 nm), UV/Vis ($\sim$ 190 – 500 nm), Vis/NIR ($\sim$ 480 – 900 nm), and IR ($\sim$ 700 – 1650 nm). For these tests, a small number of measurements were made in the VUV below 190 nm, but no signal was detected. Therefore these four cameras mostly fixed on four ranges: 190 – 370 nm (VUV), 370 – 500 nm (UV/Vis), 500 – 890 nm (Vis/NIR), 890 – 1450 nm (NIR). The data presented below are therefore considered over these ranges, or a subset of these ranges when compared to previous work.

II.A. Test Conditions

The present test campaign conditions were designed to match proposed/previous trajectories for various Titan missions and to provide invaluable data for correctly simulating the radiative heat flux and quantifying uncertainty margins. Tests were designed to match conditions from previous EAST campaigns (2003 – 2005) and tests conducted in the X2 facility in Australia.[2] Furthermore, a small number of tests also focused on validating higher shock speeds to open the trajectory space available to future Titan mission planners. Figure 1 shows a plot of various proposed and previously flown Titan entry trajectories with the Test 61 conditions. These conditions correspond to a shock speed range of 4.7 to 8 km/s, free stream pressures of 0.1 Torr (13.3 Pa), 0.28 Torr (37.2 Pa) and 0.47 Torr (62.5 Pa) and a test gas composition of either 95% N_2 / 5% CH_4, 98.9% N_2 / 1.1% CH_4, 98% N_2 / 2% CH_4, 98% N_2 / 1.5% CH_4 / 0.5% Ar or 100% N_2 by mole. The 0.1 Torr condition was the focus of the current work as it has been tested by several other facilities and previous EAST campaigns. The 0.47 Torr cases are more likely to correspond to a condition close to peak heating for Titan entry.

At the time of the previous EAST campaigns (before the Huygens/Cassini mission reached Titan), there was a large degree of uncertainty regarding the composition of Titan's atmosphere, thus experiments were performed in Tests 43 & 45 at both 2% CH_4 and 5% CH_4.[1] Testing at 8.6% CH_4 was also performed in Test 43 due to a mole versus mass fraction mix up with the ordering of the test gas bottle.[1] Since the entry of the Huygens spacecraft at Titan, it was found that the CH_4 mole fraction was closer to 1.5% with trace amounts of H_2 and Ar (both less than $< 1\%$).[11] An approximate test gas composition of 1.5% CH_4 / 0.5% Ar / 98% N_2 by mole was used to replicate the Titan atmosphere in Test 61. The impact of argon on aeroheating in Titan

gas mixtures has not previously been tested experimentally or computationally. The radiation specifically from argon is likely to be small, however, argon will increase the shock layer temperature, and thus indirectly affect the radiative heating.

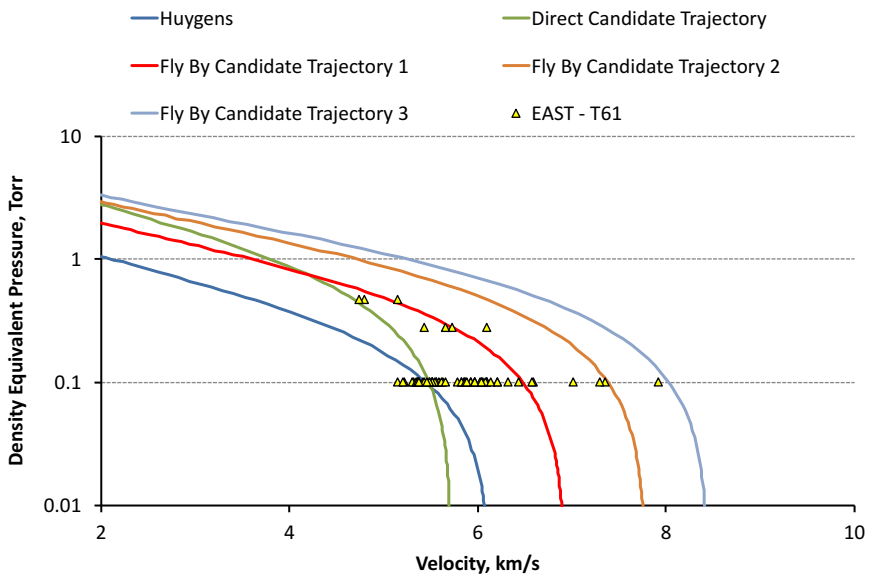

Figure 1. Comparison of EAST Test 61 testing conditions to various actual and proposed flight missions to Titan.

III. Summary of Codes

Experimental data are compared to simulations with DPLR and NEQAIR, used to calculate the flow field and radiation, respectively. This section will provide a brief overview of these codes for reference.

III.A. DPLR

DPLR[12–14] uses a finite-volume discretization to solve the reacting Navier-Stokes equations for fluids in thermochemical non-equilibrium. While the software was originally designed for steady-state aerothermodynamic analysis of planetary entry vehicles, DPLR has evolved over the years to include a broad spectrum of numerical and physical models that enable it to accurately simulate most compressible flows. Additional details on DPLR's capabilities can be found in references 12–14. The version of DPLR used in this work is v4.04.0.

A two-dimensional grid of a 3 m sphere with 805 grid points on the stagnation line was used in the DPLR solutions. The stagnation line being assumed analogous to the flow behind the shock in the EAST experiments. The simulations used a 21 species (CH_4, CH_3, CH_2, HCN, N_2, N_2^+, C_2, H_2, CH, NH, CN, CN^+, N, N^+, C, C^+, H, H^+, Ar, Ar^+, e^-)[15] gas model in the computations. In addition to chemical non-equilibrium, the flow field was assumed to be in thermal non-equilibrium as well. Consequently, a two-temperature (T_{tr}-T_{ev}) model was used. In the two-temperature model employed, the translational and rotational modes of the molecules are assumed to be in equilibrium (T_{tr}=T_{trans}=T_{rot}), and are distinct from the vibrational and electronic modes of the molecules and the temperature of the free electrons (T_{ev} =T_{vib}=T_{elec}=T_{e^-}).

III.B. NEQAIR

Non-EQuilibrium AIr Radiation (NEQAIR) is a line-by-line radiation code which computes spontaneous emission, absorption and stimulated emission due to transitions between various energy states of chemical species along a line-of-sight.[16] Individual electronic transitions are considered for atoms and molecules, with the molecular band systems being resolved for each rovibronic line. Since the report of Whiting et al.,[16] numerous updates have been incorporated into NEQAIR, such as: using the latest version of the NIST atomic database (version 5.0),[17] using the bound-free cross sections from TOPbase,[18] incorporating the CO_2

database from CDSD-4000,[19] parallelization and improvements to the mechanics of the Quasi Steady State (QSS) model. Of particular relevance to this paper was the implementation of a QSS model for CN.[20,21]

The current release version of NEQAIR is known as v14.0.[22] However, due to further improvements to QSS and fixing spurious radiation from atomic nitrogen in the IR, N_2 1st Positive and N_2^+ 1st Negative under certain conditions, the pre-release of v15.0 has been used for the calculations presented in this paper. An over-prediction by atomic nitrogen in the IR was previously noted to be due to use of the excitation rates of Park.[23] In an attempt to reduce the effect of the over-prediction, a merged database of the rates from Huo and Park has been created and discussed by Cruden and Brandis.[24] The merged database appears to have mitigated the issue of providing an over-prediction for atomic transitions. In this work, radiance from hydrogen atoms was not simulated. NEQAIR does not have a non-Boltzmann model for hydrogen and the radiance predicted for Boltzmann distributions were so large as to provide erroneous integrated radiances. As there is no evidence of emission in the EAST spectrum from hydrogen (e.g. from the H-alpha line) except at the highest velocity conditions, this approximation is acceptable.

IV. Non-equilibrium Analysis Methodology

Insights into the agreement between simulations and experimental results for high-speed Earth entry radiation were made possible by analyzing integrated equilibrium spectra across a wide range of conditions and conducting detailed comparisons of the resulting trends.[25,26] For non-equilibrium flows, however, it is not immediately clear that one parameter can describe the non-equilibrium intensity observed in several shots over a large range of conditions. The temporal intensity changes significantly with shock speed as a result of the underlying change in the physics. The benefits and drawbacks of three proposed methods for determining a parameter that highlights either the relative significance of the non-equilibrium radiative intensity or the absolute intensity emitted in the non-equilibrium region were previously analyzed.[27] The goal of such a parameter is to enable the comparison of several simulations and experimental results. Of these three methods, the absolute non-equilibrium metric is used in this work. This metric is computed by integrating the radiance within 2 cm of either side of the radiative peak, as shown by the red lines in Fig. 2, and is normalized by the shock tube diameter. Computing the metric in this manner has been suggested as a more robust way to conduct a comparison as opposed to using the peak intensity, since the comparisons are then not dependent upon experimental resolution limitations such as gate opening times and spatial smearing due to shock movement. Under optically thin conditions, this integral will represent the radiance as observed parallel to the direction of the shock. Under optically thick conditions, however, this integral has no additional physical meaning and is simply a way of comparing data corresponding to a given optical path-length/shock tube diameter. Previous analyses of Titan non-equilibrium radiation were reported using the peak intensity as the metric for comparison.[2,3] As such, some comparisons of the present work to previous data have been conducted in this manner.

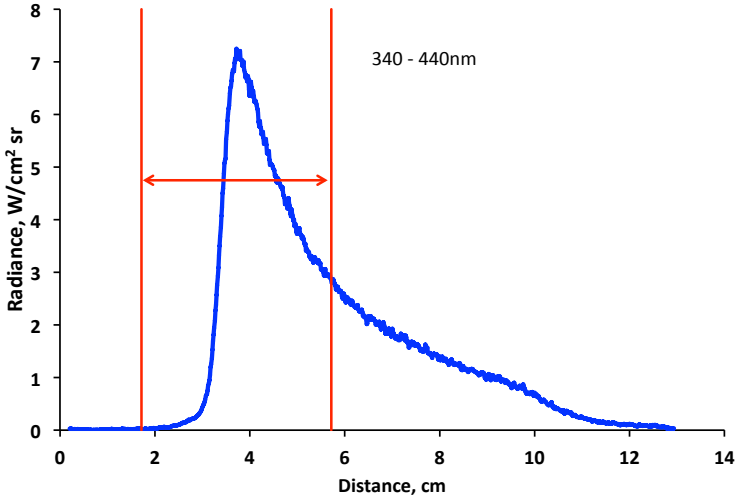

Figure 2. Example of the "Absolute Non-equilibrium Radiance" metric to be used in this work: Integrating the intensity from 2 cm before the shock peak until 2 cm after the shock peak.

V. Results and Comparisons

The results of the Titan experiments performed in the recent EAST test campaign will be presented in multiple ways, with comparisons against simulations and other experimental data shown where appropriate. The experiments are plotted using the non-equilibrium metric across the four spectral ranges that are typically used during EAST experiments, as shown in Fig. 3. The data are shown for several different variations in methane concentration. Comparisons are also shown with DPLR/NEQAIR simulations, which were performed after the test was completed. The level of agreement between simulations and experiments is very good across the VUV, UV/Vis and IR spectral ranges, generally within 30%. Even though good agreement is observed, there is a substantial under-prediction in the Vis/NIR spectral region. It is suspected that the reason for the reduced agreement in this range could be due to an issue with the non-Boltzmann modeling of CN Red. A less significant under-prediction is also observed in the IR spectral range. The agreement with NEQAIR is generally best at the highest (8.6%) and lowest (0%) CH_4 concentration. The better agreement is likely due to a lower uncertainty in the composition of the test gas with either larger CH_4 percentage or pure N_2. Because the test gas is mixed dynamically with mass flow controllers, the uncertainty in the CH_4 fraction is approximately 0.2% regardless of the composition, which is a much larger relative error when the CH_4 fraction is low. The test gas composition is confirmed by conducting Residual Gas Analyzer (RGA) readings prior to each experiment. Even though small shot-to-shot variations in the test gas composition were observed, any deviation this caused in the radiation measurements was within the noise of the data. The good level of agreement shown with the 100% N_2 data indicates that there is minimal emission from contamination species (in particular, CN).

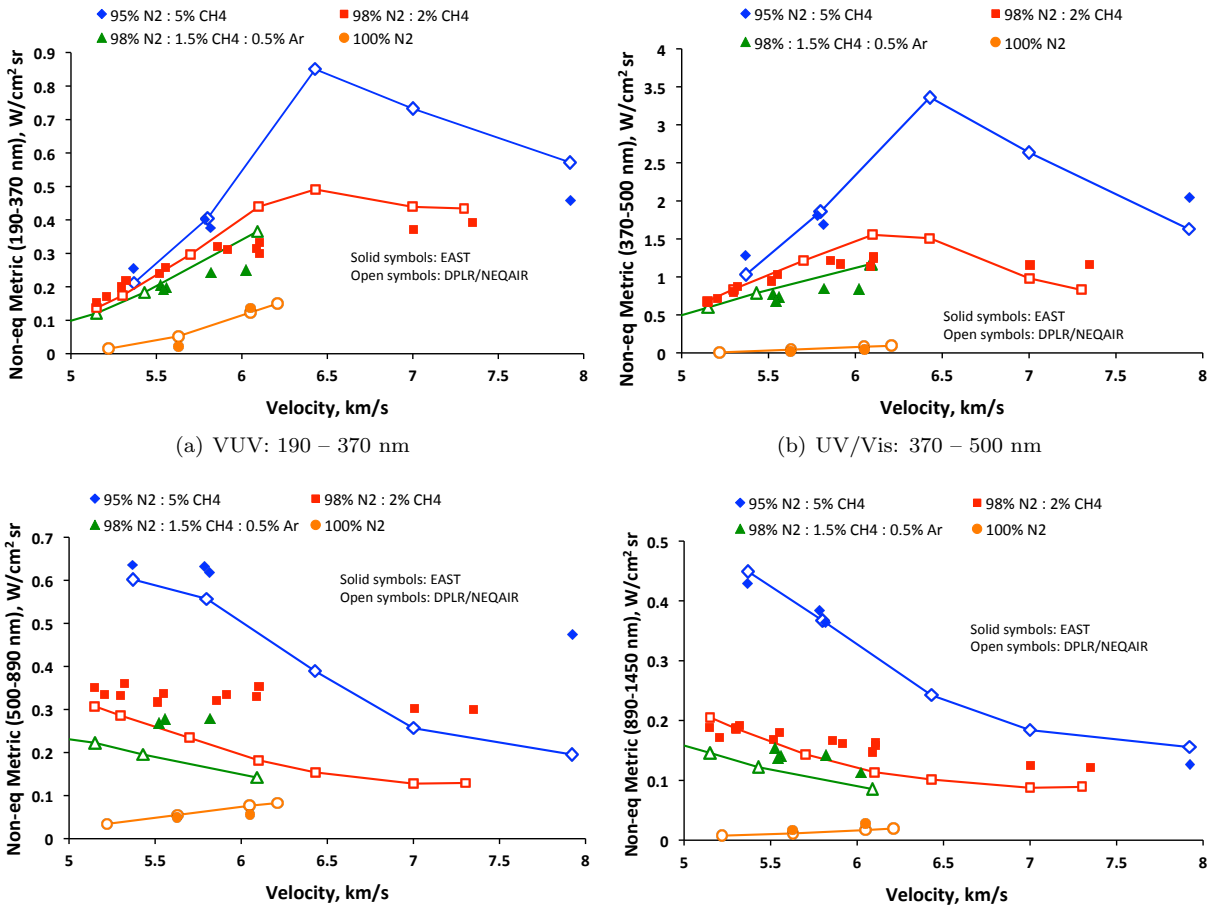

(a) VUV: 190 – 370 nm

(b) UV/Vis: 370 – 500 nm

(c) Vis/NIR: 500 – 890 nm

(d) IR: 890 – 1450 nm

Figure 3. Non-equilibrium metric radiance at different compositions of CH_4, N_2 and Ar at 0.1 Torr.

V.A. Comparison with Previous Shock Tube Data

Results from the recent campaign, Test 61, have been compared with previous Titan experiments performed in EAST, Tests 43 & 45. Tests 43 & 45 were performed prior to the facility upgrade in 2008. The non-equilibrium metric has been used to compare the experimental and simulation results as shown in Figs. 4 to 7. Wavelength regions have been chosen to maximize the number of tests than can be used for comparison across Tests 43, 45 and 61. Figure 4 shows results for 100% N_2, Fig. 5 shows results for 98% N_2 / 2% CH_4, Fig. 6 shows results for 95% N_2 / 5% CH_4 and Fig. 7 shows results for 91.4% N_2 / 8.6% CH_4. The results presented in Figs. 4(a) and 4(b) should indicate if there is significant carbon contamination, as these plots correspond to the range where CN Violet would emit if present in the shock tube. As the figures show that the non-equilibrium metric results are generally similar in magnitude for both Test 45 and 61, and are less than the DPLR/NEQAIR simulations, the level of carbon contamination is likely small, and consistent between both test series. However, as shown in Fig. 4(b), it appears that there is significant contamination emission found in Test 43.

Figure 5 highlights that there is a significant discrepancy between Test 61 and Test 45, with Test 61 being 2 to 4 times larger in magnitude compared to Test 45. Even though there is a significant discrepancy, the trends with velocity between the two data sets are similar. The data from Test 43 shows no discernible trend, as shown in Fig. 7, therefore comparisons with previous EAST data will focus on Test 45. For most velocities and variations of CH_4 concentration, the simulations agree far better with Test 61 data. The exception being that for the higher speed shots at 98% N_2 / 2% in the 480 to 680 nm range, the simulations agree better with Test 45 (see Fig. 5(c)). However, as will be noted later in the paper, the spectral comparison is substantially improved when the simulations are compared to Test 61 as opposed to Test 45.

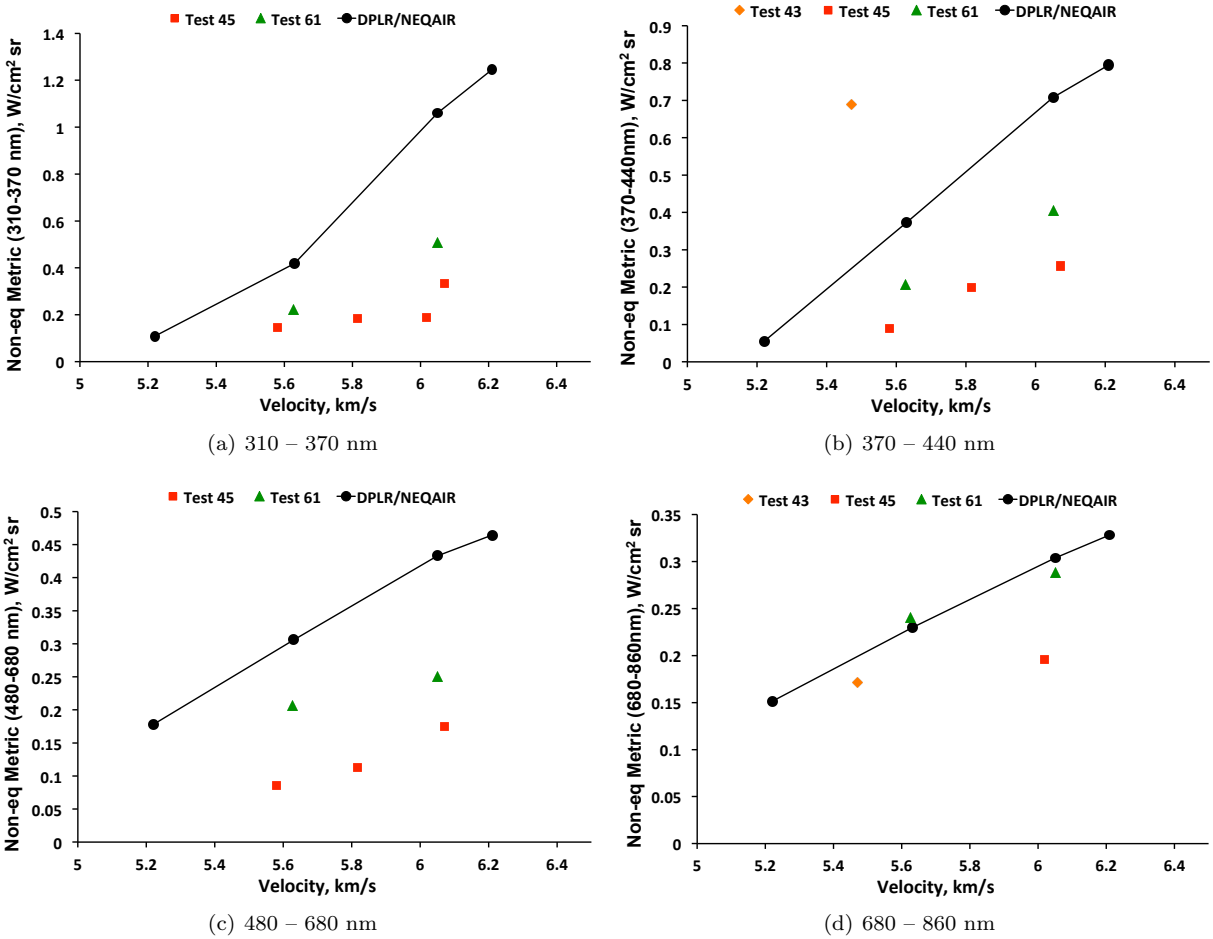

(a) 310 – 370 nm

(b) 370 – 440 nm

(c) 480 – 680 nm

(d) 680 – 860 nm

Figure 4. Non-equilibrium metric comparison at 100% N_2, 0.1 Torr.

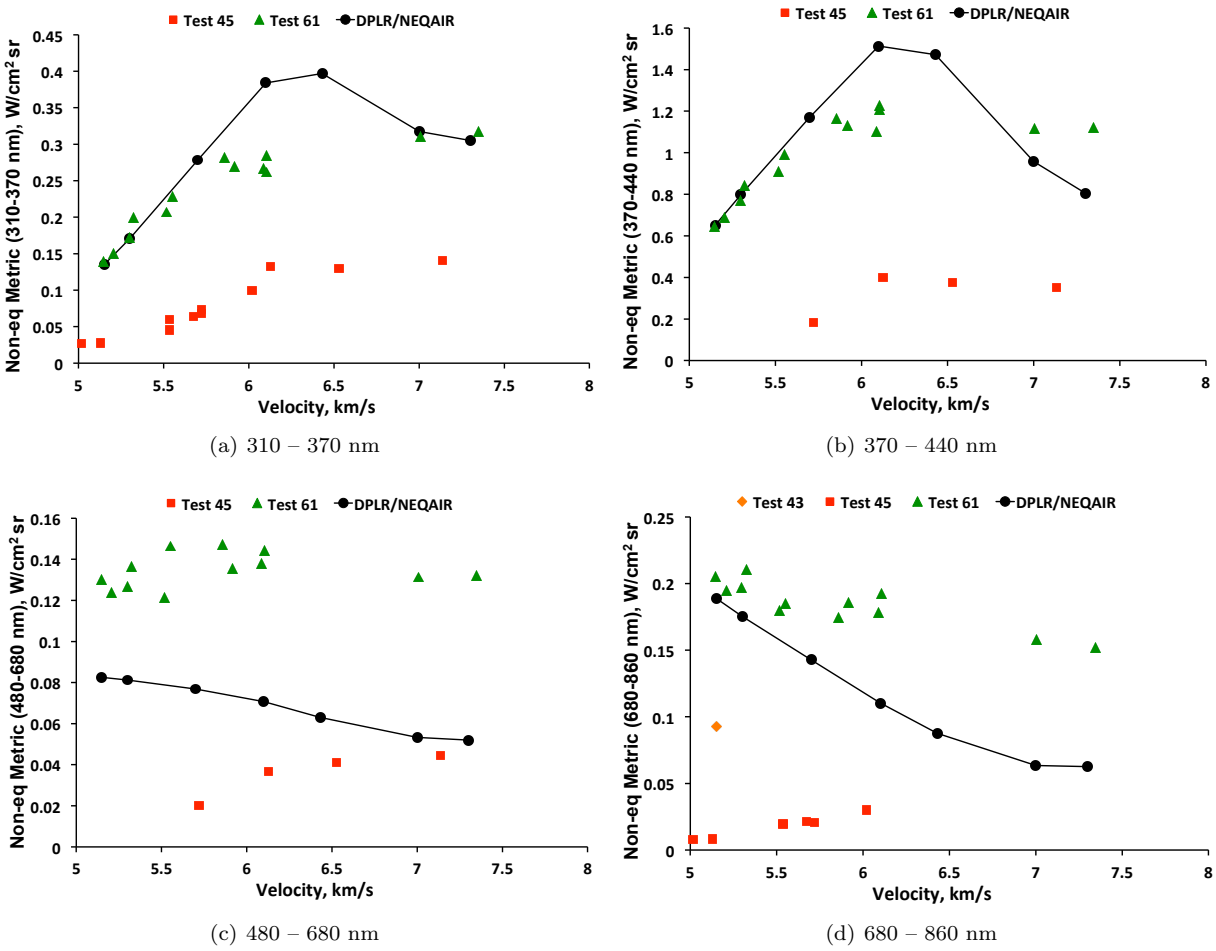

(a) 310 – 370 nm

(b) 370 – 440 nm

(c) 480 – 680 nm

(d) 680 – 860 nm

Figure 5. Non-equilibrium metric comparison at 2% CH_4 / 98% N_2, 0.1 Torr.

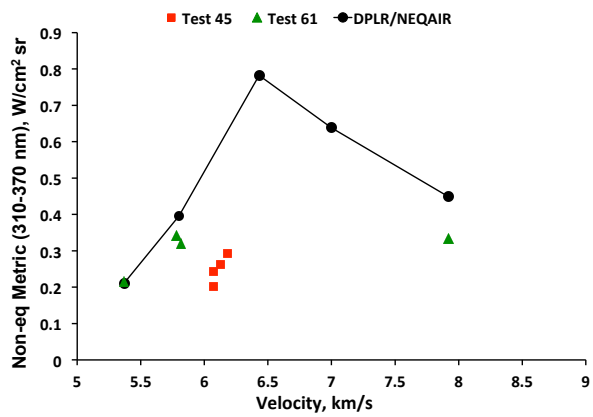

(a) 310 – 370 nm

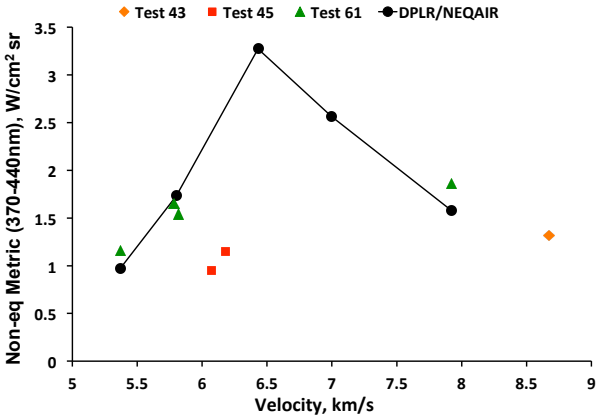

(b) 370 – 440 nm

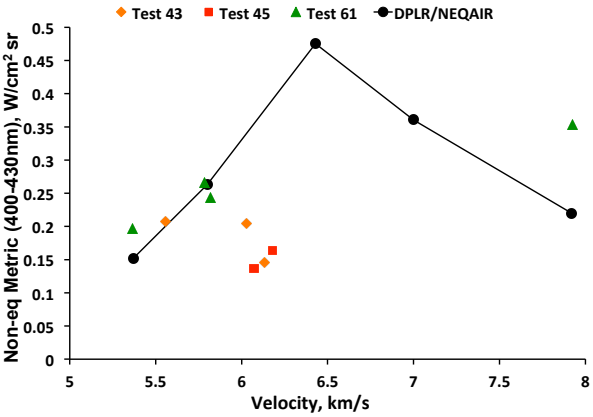

(c) 400 – 430 nm

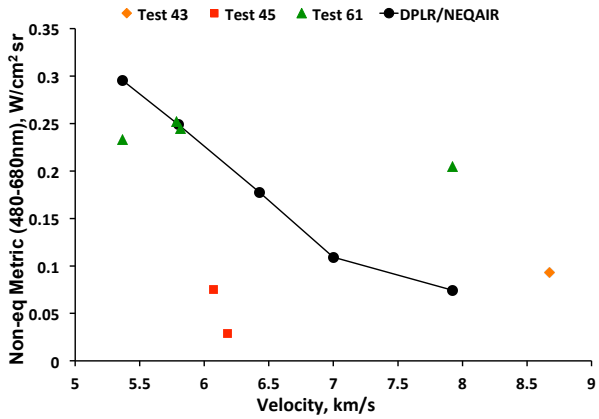

(d) 480 – 680 nm

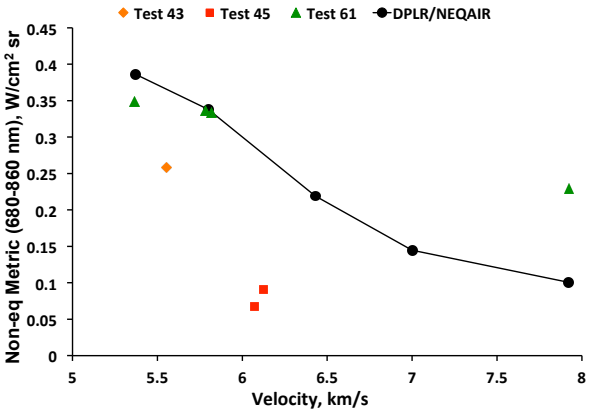

(e) 680 – 860 nm

Figure 6. Non-equilibrium metric comparison at 5% CH_4 / 95% N_2, 0.1 Torr.

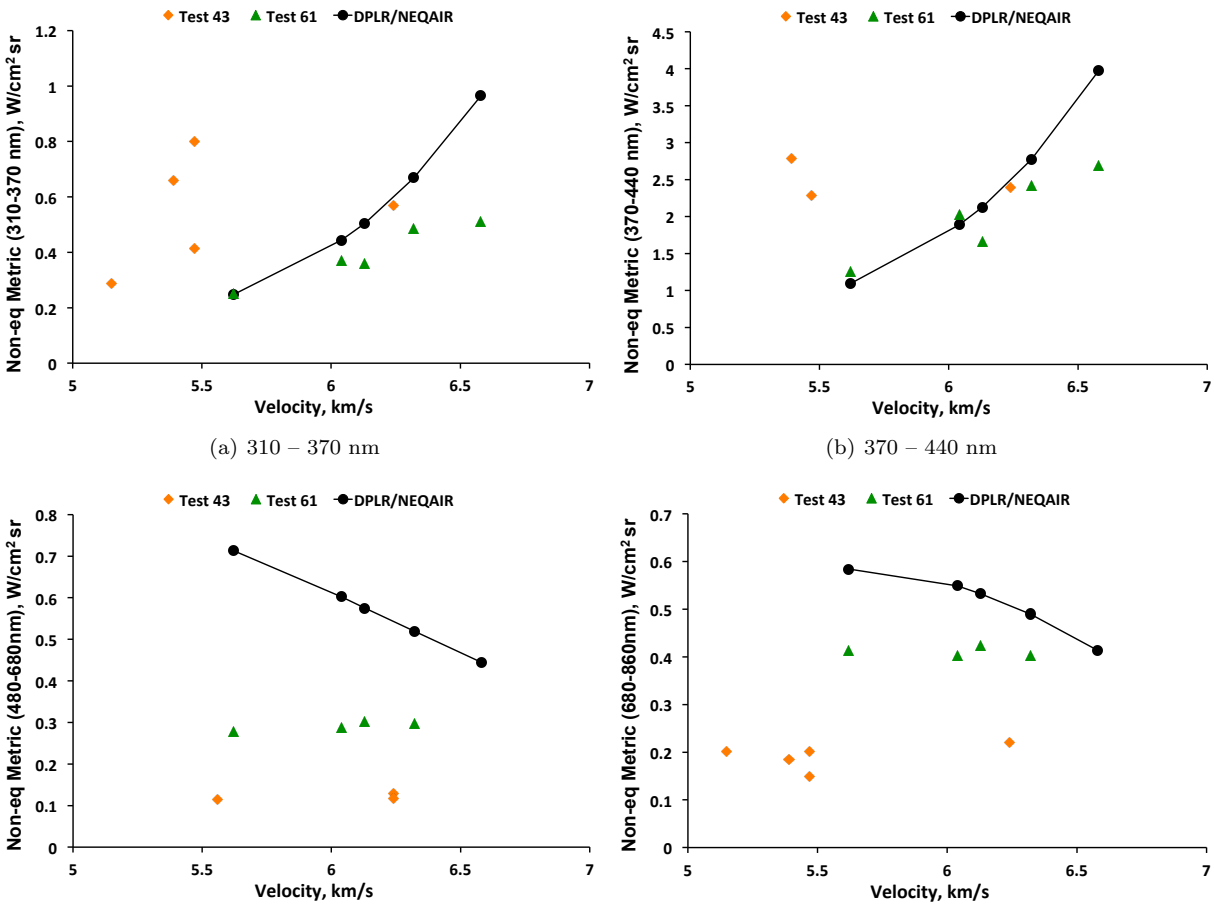

(a) 310 – 370 nm

(b) 370 – 440 nm

(c) 480 – 680 nm

(d) 680 – 860 nm

Figure 7. Non-equilibrium metric comparison at 8.6% CH_4 / 91.4% N_2, 0.1 Torr.

Figure 8(a) shows the comparison of a radiance profile from Test 61, Test 45 and DPLR/NEQAIR at approximately 6.1 km/s, 98% N_2 / 2% CH_4 and 0.1 Torr in the UV spectral region. The figure shows that the DPLR/NEQAIR result compares very well in terms of the peak radiance magnitude with the Test 61 data. The Test 45 peak radiance is about a factor of 4 lower compared to either Test 61 or DPLR/NEQAIR. The figure also shows that there is a significant disagreement between the experimental and simulated decay rates, with the simulation showing a slower decay. Figure 8(b) shows a plot of radiance normalized by the peak value. Even though the radiance magnitudes for Test 45 and 61 are quite different, the figure shows that both experiments have very similar decay rates. Figure 8(c) shows a plot of the non-equilibrium metric spectral radiance and due to the slower decay rate, the simulated value is larger compared to Test 61.

The decay rate in a Titan atmosphere is largely controlled by the rate of nitrogen dissociation ($N_2 + M \Longleftrightarrow N + N + M$) coupled with the exchange reaction ($N_2 + C \Longleftrightarrow CN + N$).[28] It was previously reported that by increasing the nitrogen dissociation rate improved agreement with the decay rate,[28] and this is shown to be the case with the new data, see Fig. 9(a). The figure shows that excellent agreement in the decay rate is observed when the nitrogen dissociation reaction is increased by a factor of 3 (listed as "N2x3" in the figure legend). Increasing the nitrogen dissociation reaction by a factor of 3 is probably at,[15] or maybe even beyond, a reasonable uncertainty bound for this rate. Furthermore, recent quantum chemistry calculations suggest that at these temperatures the Park rate provides an over-prediction,[29] indicating that some other phenomena, such as the CN non-Boltzmann modeling, might be at play. Figure 9(b) shows the impact of applying a Boltzmann state population to the radiation simulation. While increasing the nitrogen dissociation rate reduces the peak radiance, the Boltzmann calculation shows that the peak radiance is approximately a factor of 3 higher compared to the experiment. This over-prediction by the Boltzmann distribution allows for the possibility that the non-Boltzmann model is incorrectly predicting the CN(B) state population that is responsible for CN Violet radiation.

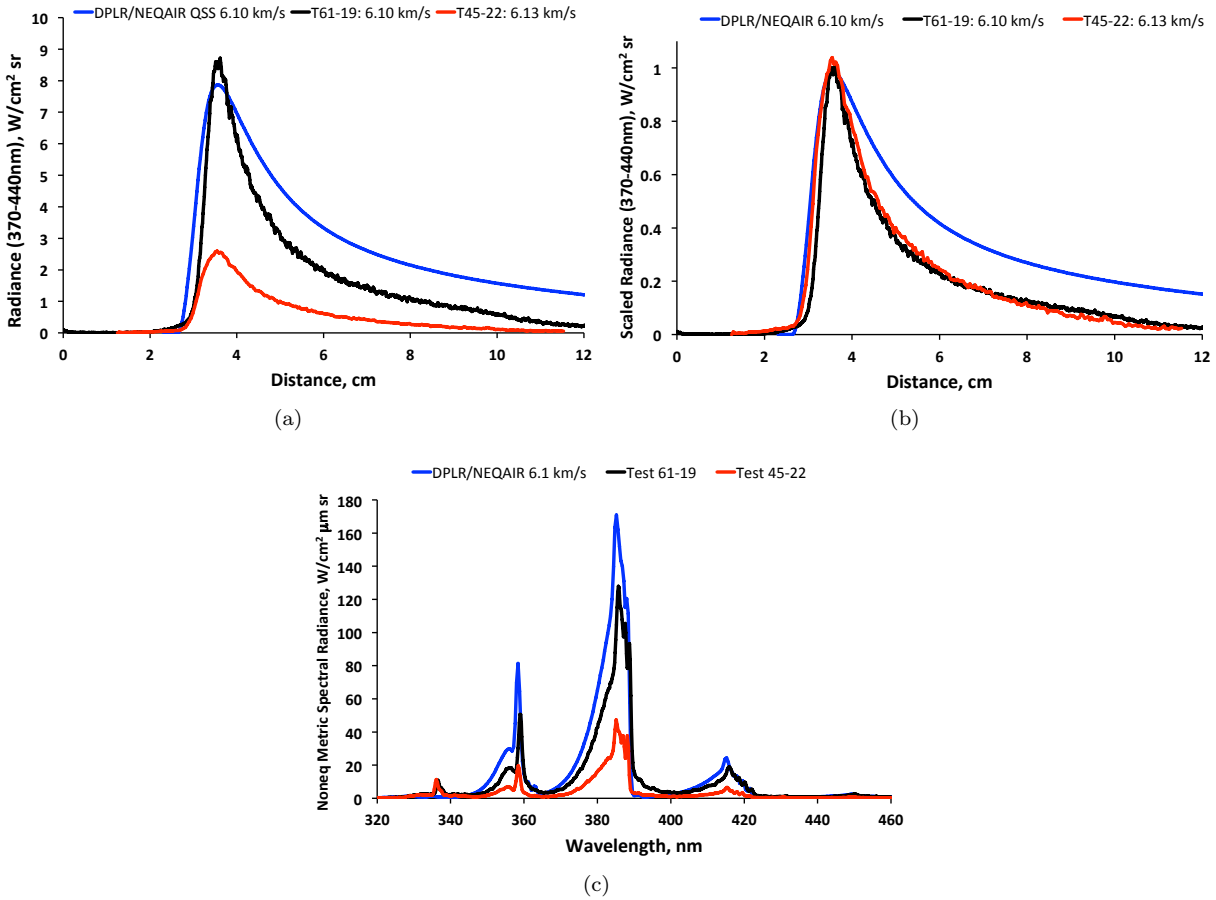

Figure 8. Simulations compared with Test 61 and Test 45 data at 2% CH_4 / 98% N_2, 0.1 Torr and ~6.1 km/s.

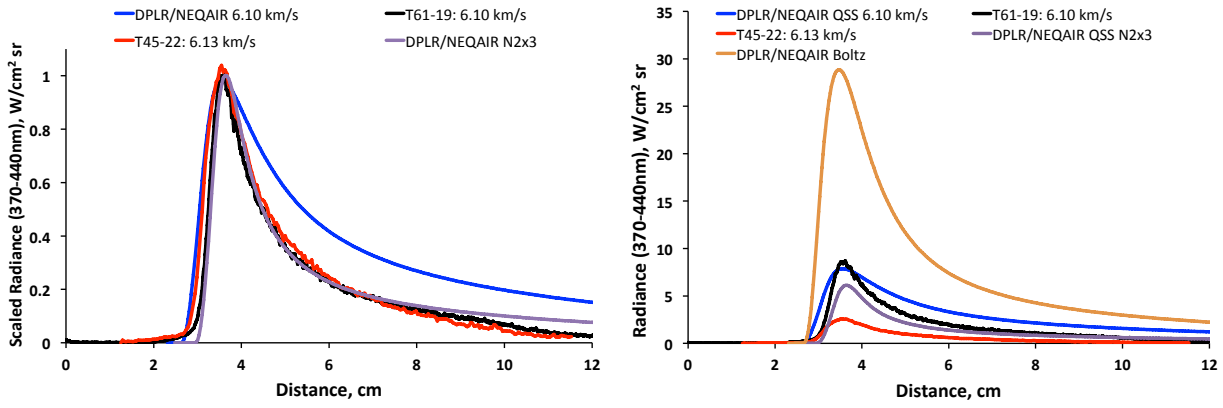

(a) (b)

Figure 9. Variations in simulations to modify peak magnitude and decay rate.

Figure 10(a) shows a radiance profile comparison of Test 61, Test 45 and DPLR/NEQAIR at approximately 6.1 km/s, 98% N_2 / 2% CH_4 and 0.1 Torr in the Vis/NIR spectral region. The figure shows that in terms of the peak radiance, the DPLR/NEQAIR result is approximately a factor of 1.7 less than Test 61 and approximately a factor of 2.5 times larger than Test 45 in terms of the peak radiance magnitude. However, unlike the UV spectral region, the figure shows that the experimental and simulated decay rates are very well matched. The excellent agreement for the radiance decay rate is highlighted by the normalized radiance shown in Fig. 10(b). Figure 10(c) shows the impact of applying a Boltzmann state population to the radiation simulation. As with the UV spectral region, the Boltzmann distribution provides a substantial over-prediction. This over-prediction by the Boltzmann distribution allows for the possibility that the non-Boltzmann model is under-predicting the CN(A) state population that is responsible for CN Red radiation. From Fig. 10(d), which shows a plot of the non-equilibrium metric spectral radiance, it is clear that the CN Red radiance is under-predicted by the simulation. Even though there is no non-Boltzmann model for C_2 in NEQAIR, good agreement is observed between the Test 61 results and the simulations for C_2 Swan (480 - 520 nm).

A comparison of the data obtained in the X2 shock tube with EAST results is shown in Fig. 11. Two sets of data are shown for X2, and correspond to testing with different shock tube materials and diameters. The results labeled "X2 AB"[2] used a steel tube with a diameter of 8.5 cm, while the results labeled "X2 CJ"[3] used an aluminum tube with a diameter of 15.5 cm. The data are presented in terms of peak radiance, as this was the metric applied in the previous studies.[2,3] In the case of Titan entries, relaxation is slow enough in comparison to the shock motion and camera gating time so as to be comparable across different facilities, though this is not generally true of all shock tube tests. As can be seen in the figure, results from X2 and Test 45 are relatively consistent. When compared to the new EAST data (Test 61), there is a significant discrepancy in the peak radiance, up to a factor of 10. This discrepancy was examined in more detail, varying many testing parameters and procedures in an attempt to resolve the difference. Factors investigated include absolute intensity calibration, methods for filling the test gas into the tube, methods for mixing the test gas and the purity of the test gas. Several of these factors are shown in Fig. 11 and are discussed in Sect. VI. The level of contamination in each X2 test campaign was reported, and these values were used to determine the amount of air added to the Titan test gas in Test 61 for a small number of shots. The addition of 1.4% O_2 significantly reduced the peak radiance, by about 40%, but was not enough to fully explain the difference. Further tests were tried with doubling the O_2 added to 2.8%, or trying 1.1% CH_4 with 1.4% O_2, but these tests still did not completely agree with the X2 or Test 45 results. Figure 11 also shows results from DPLR/NEQAIR, and excellent agreement can be seen with the Test 61 data. Results from CR models,[1–3,8,9] which were benchmarked to previously reported data, may now provide under-predictions when compared to Test 61.

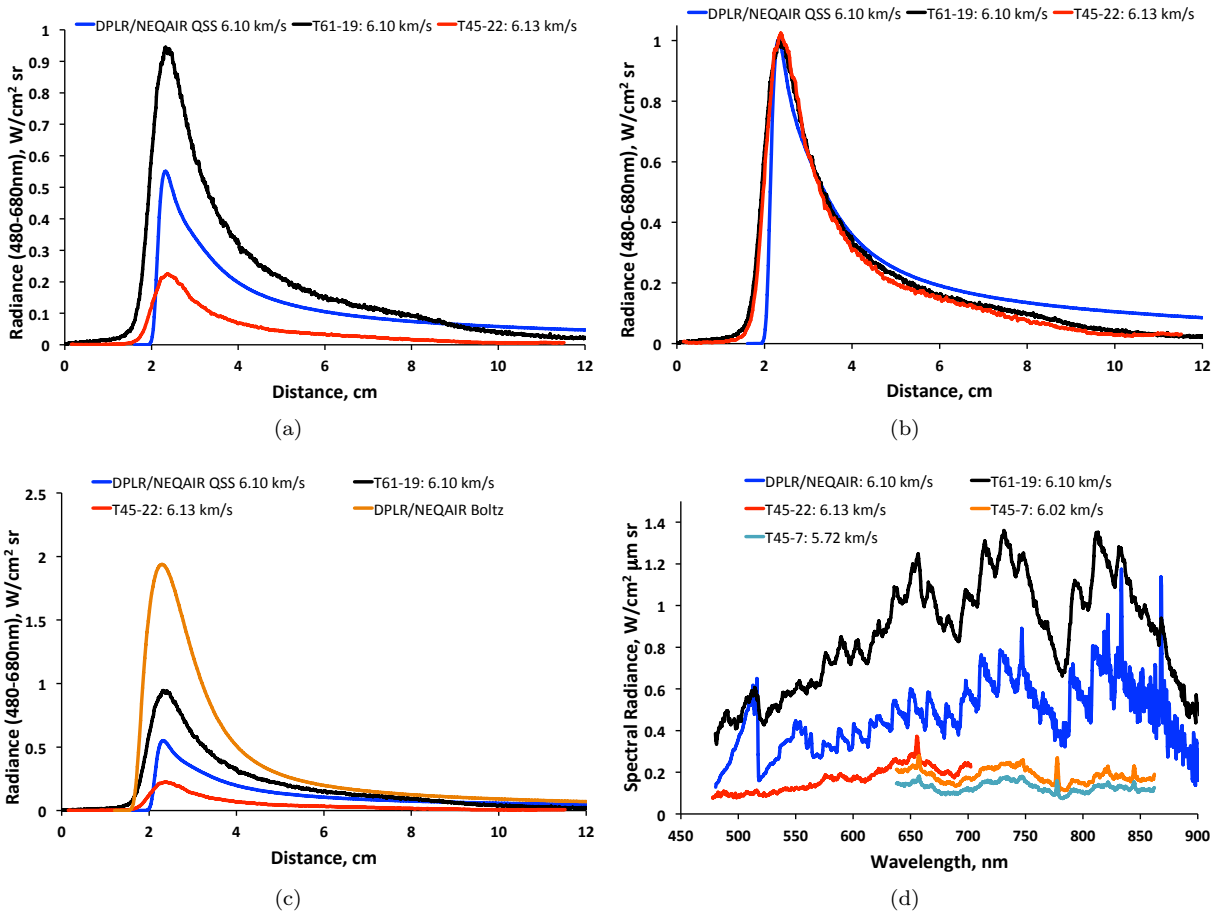

Figure 10. Simulations compared with Test 61 and Test 45 data at 2% CH_4 / 98% N_2, 0.1 Torr and ~6.1 km/s.

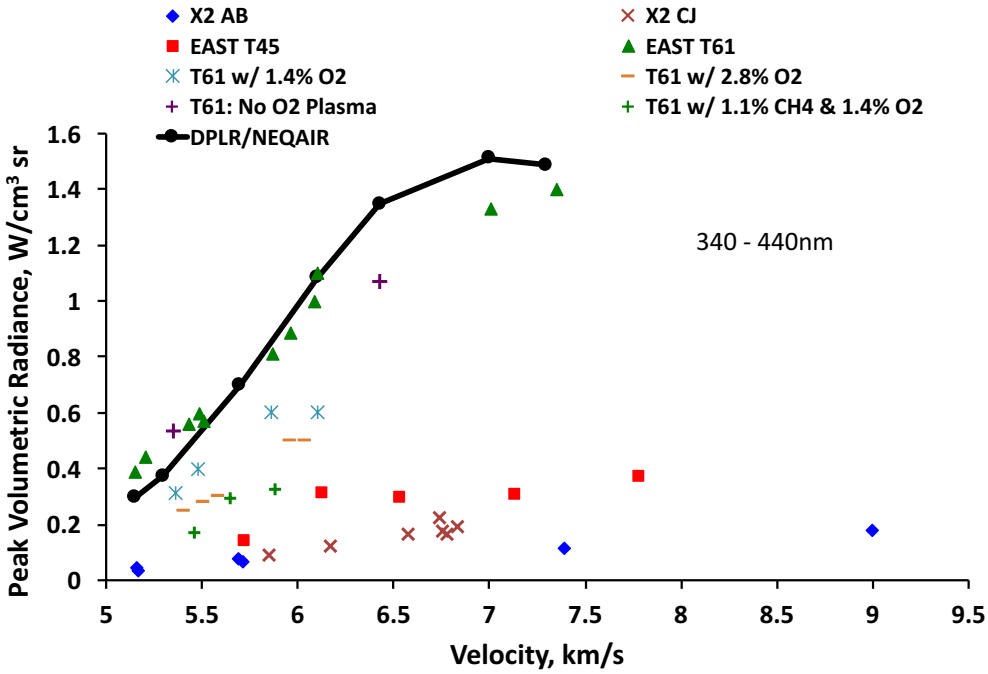

Figure 11. Comparison of multiple X2 test campaigns (X2 AB, X2 CJ) with results from EAST tests 45 and 61.

V.B. Validation of Calibration with High-Speed Nitrogen

In order to confirm the calibration procedure used in Test 61, two high-speed pure nitrogen shots were performed with the same experimental set-up. The high-speed condition was chosen to ensure that the shock comes to equilibrium and because EAST has previously demonstrated good agreement to equilibrium at these conditions.[25] Results for the UV/Vis and Vis/NIR spectral regions are shown in Fig. 12. These regions cover the spectral ranges of the dominant Titan radiators of CN Violet, CN Red and C_2 Swan. The figure shows that very good agreement is obtained between the EAST results and NEQAIR calculations based on CEA[30] equilibrium, within 7% for the UV/Vis and within 2% for the Vis/NIR. This excellent level of agreement increases confidence in the EAST Test 61 calibration.

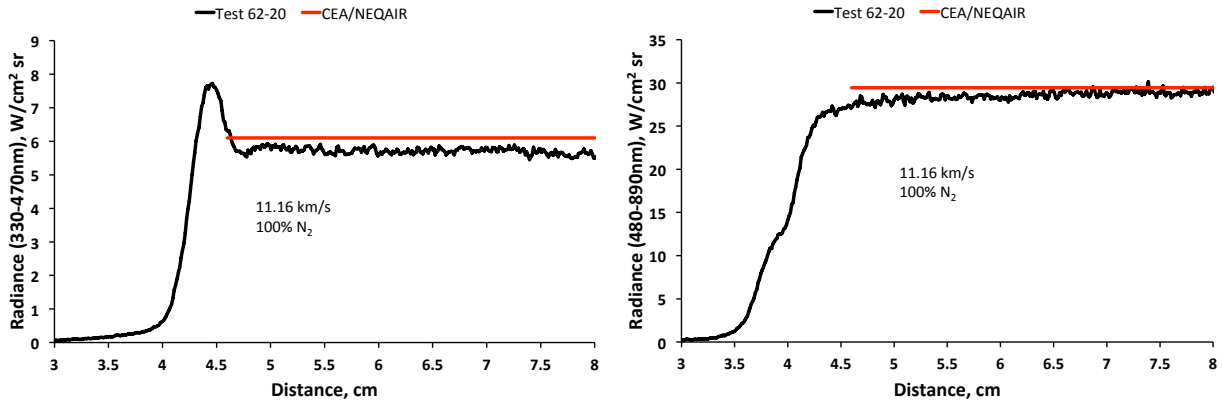

(a) UV/Vis (b) Vis/NIR

Figure 12. Radiance measured at 100% N_2, 11.16 km/s, 0.1 Torr compared with equilibrium.

VI. Examination of Discrepancies

As was evidently clear in the previous section, there are significant discrepancies between the new experiments and the previously published data. Therefore, a significant effort was undertaken to investigate potential reasons for this discrepancy, with the hope of being able to re-create the old EAST experiments. These efforts are broken up into two sections. Section VI.A discusses different modes of facility operation and Sect. VI.B discusses contamination and calibration issues.

VI.A. Facility Operation

Due to the significant discrepancies between the Test 61 and Test 45 data, tests were performed with the goal of temporarily stripping back some of the facility upgrades that occurred in 2008. Two of the upgrades that were speculated to have an effect on the radiance measurements were the method of gas loading and mixing the test gas and the use of an oxygen plasma cleaner. Previous works have shown that the oxygen plasma cleaner is very successful at reducing carbon contamination in the facility.[4]

The current gas loading configuration uses mass flow controls to meter the gas into the facility just prior to the shot. This gas loading method allows the gas to be mixed dynamically and ratios to be specified with greater flexibility, as opposed to using pre-mixed tanks. Consequently, the delay time between the facility loading and shot firing is shortened, which should reduce contamination levels due to outgassing and facility leakage. Three variations for filling the test gas were attempted in order to reproduce previous test conditions. The first method used a single mass controller with an externally supplied pre-mixed tank of 98% N_2 / 2% CH_4 by mole (listed as "Pre-mixed" in the figure). The "Pre-mixed" shots would still retain a short delay to fire, but may impact the control of the gas ratio during loading. The second method bypassed the gas loading system, and manually loaded the gas directly into the tube (listed as "Manual load" in the figures). The "Manual load" shots would have a longer delay time than the first method (which used the mass flow controller). The third method was the same as the second method, except the manually filled test gas was allowed to sit in excess of 10 minutes prior to the shot (listed as "Manual w/Delay" in the figures). A final variation combined the manual load process and disabled the oxygen plasma cleaner prior to the shot

(listed as "No O2 plasma" in the figures). This variation would have been the most similar to the practices employed in Test 45, even though it would not replicate any build up of contaminants over time. Figure 13 shows the results of these experiments. None of these variations showed a significant enough effect to bring the results in line with the Test 45 data. For the most part, data from these tests were within the noise of the experiment. Arguably, there might be some reduction in radiance in the Vis/NIR region at low velocities when the variants based on manual loading were employed. However, more shots would be needed to verify if this phenomenon is real.

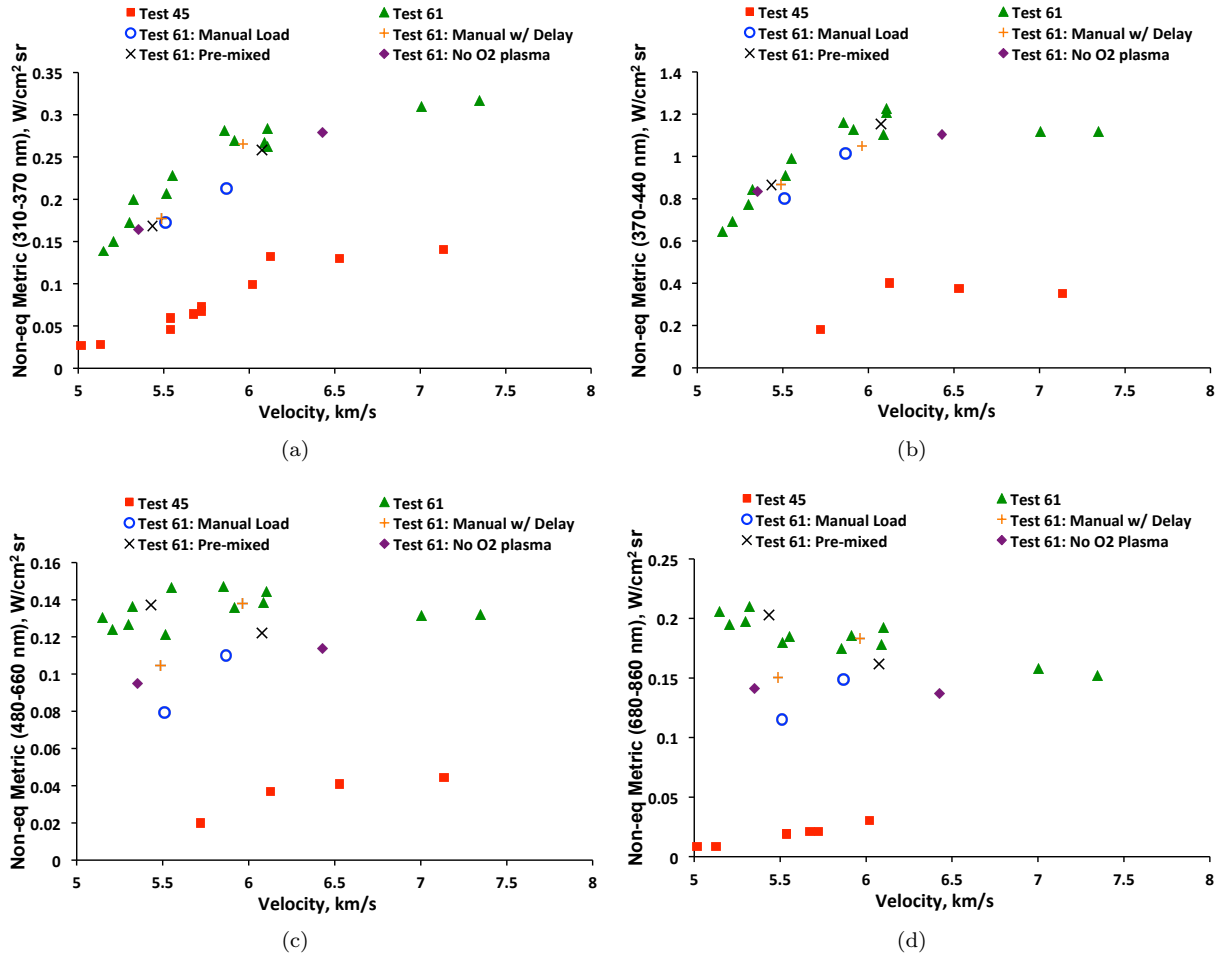

Figure 13. Non-equilibrium metric comparison at 2% CH_4 / 98% N_2, 0.1 Torr with experimental variations.

VI.B. Contamination and Calibration Issues

Previous reports have identified potential calibration and contamination issues with pre-upgrade EAST results (before 2008).[4] These issues could contribute to the discrepancy. It has been reported from test campaigns in X2 that a small amount of air leakage occurs after isolating the vacuum pumps and before firing the test.[2,3] This amount of air might initially appear small, as it is mostly nitrogen, as is the atmosphere of Titan. However the addition of oxygen can be very significant as it will react with the CH_4 to form CO and thereby reduce the carbon available to form CN. To a lesser extent, the oxygen will also react with N_2 to form NO and thereby reduce the nitrogen available to form CN. Equilibrium simulations of these shock conditions show that a small amount of oxygen (1.4%) can reduce the equilibrium CN number density by as much as a factor of two. As an example, based on CEA[30] equilibrium calculations, the mole fraction of CN is reduced by 40% for a 5.7 km/s and 0.1 Torr condition when 1.4% of O_2 is added. Therefore, air was deliberately added to the EAST test gas to assess this effect. Air was added to provide molar percentages of O_2 at 1.4% and 2.8%. The lower of these two levels was chosen to match the reported air leakage in the X2

facility,[3] and the higher level was selected as an over-test of the air leakage issue. As shown in Sect. V.A, the addition of air resulted in a significant reduction in CN radiance, but not enough to explain the discrepancy.

An additional test examined the possibility of having an incorrectly mixed gas bottle during the campaign. While this seems unlikely given that gas bottles are tested and certified by the supplier, there is precedence for errors of this nature. In EAST Test 43, a 5% CH_4 mixture by mass was received from the supplier when the tank was expected to be mixed by mole. In Test 61, it was discovered that a pre-mixed tank containing a 2% CH_4 methane mixture had a 0.1% Ar impurity. These type of mistakes would be discovered during testing in the current facility operation due to RGA characterization of the test gas performed during every shot. However, prior to 2008, no such instrumentation was in use. In the later stage of Test 43 and in Test 45, the tank was specified as 1.1% CH_4 mixture by mass, which is equivalent to 2% by mole. A few tests were performed using 1.1% CH_4 (by mole) with a 1.4% O_2 impurity added. This test was intended as an extreme case of errors in the gas mixture.

The results of the air addition tests are shown in Fig. 14. The figure shows that a small amount of O_2 causes a significant difference, reducing the radiation by almost a factor of 2. The extreme cases of 2.8% O_2 or 1.1% CH_4 with 1.4% O_2 produced even lower radiances and are getting close to the reported radiation from Test 45. However, even with this unlikely combination of factors, its still does not fully explain the discrepancy. The discrepancy can seemingly only be explained by a combination of multiple effects, including contaminants in the test gas used in the previous experiments, radiance calibration issues and inaccuracies in shock speed measurements. The accuracy in measuring shock speed in EAST improved after the facility upgrade due to there being more pressure transducers installed in the facility, sampling at a higher rate and the use of a more robust technique for calculating the shock speed. The accuracy in shock speed for Tests 43 and 45 was quoted to be 1.5%, while the current uncertainty is up to 0.4%.[4] It was not possible to reproduce the combination of effects required to exactly match Test 45 or X2 data during the Test 61 campaign.

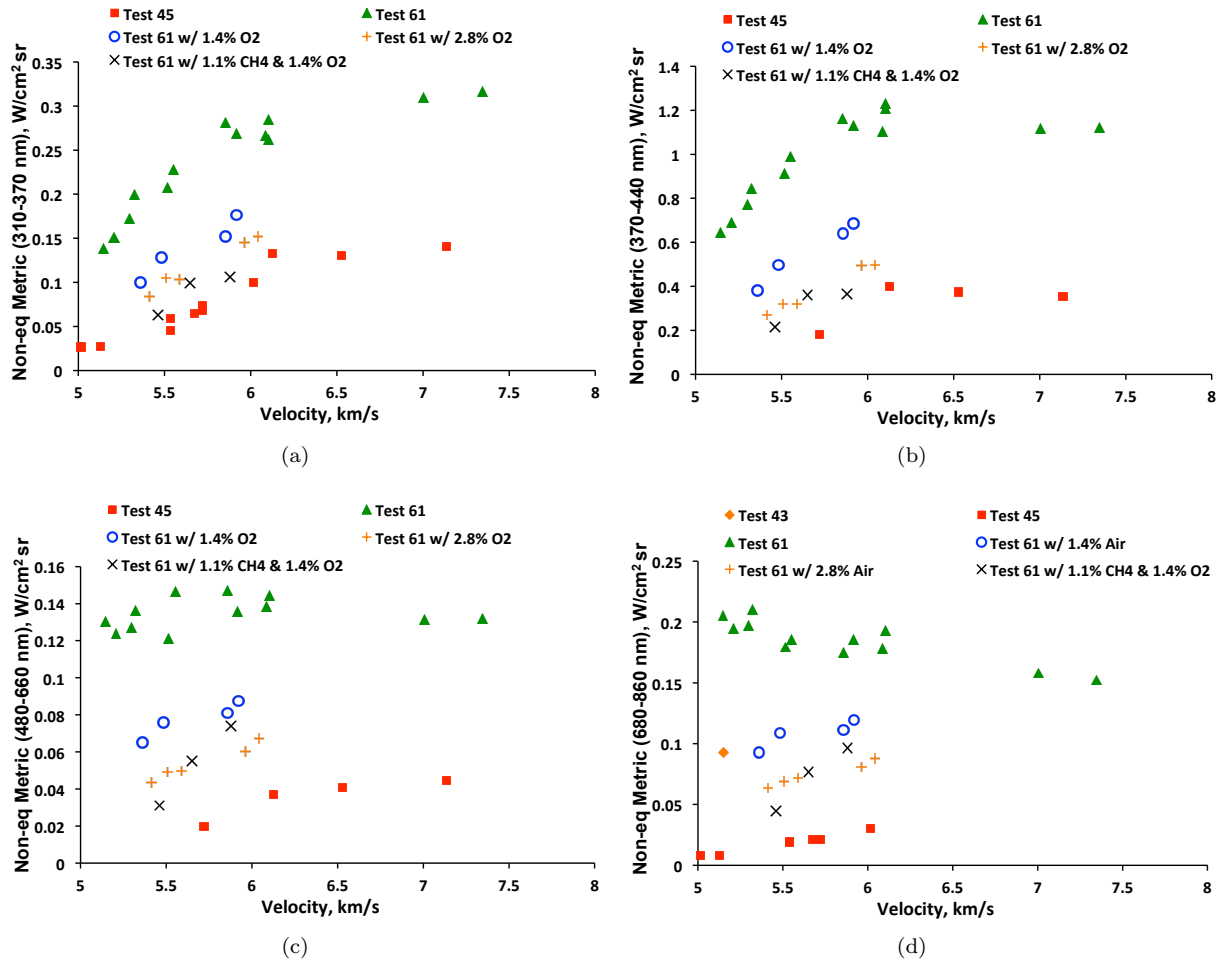

Figure 14. Non-equilibrium metric comparison at 2% CH_4 / 98% N_2, 0.1 Torr with attempts to recreate previous data.

VII. Selected Data for Validation

This section will detail selected experiments from the EAST Test 61 campaign for use in future model validation and experimental comparison. The spatially and spectrally resolved radiance is shown for a variety of conditions. The 2% CH_4 / 98% N_2 results are shown in this section, with more details and other compositions presented in the Appendix. These selected data sets were chosen based on consistency with other results from Test 61 combined with good experimental characteristics, such as test time. Figure 15 shows three experiments at 5.15 km/s, 6.1 km/s and 7.35 km/s across the four spectral ranges measured in EAST. Figures 16(a) and 16(b) show the non-equilibrium metric spectral radiance for the UV/Vis and Vis to IR spectral regions respectively. Figure 16(c) shows a composite non-equilibrium metric spectral radiance at 5.15 km/s across all four spectrometers. The relative importance of CN Violet is clearly seen in this figure, contributing to over 60% of the total radiance.

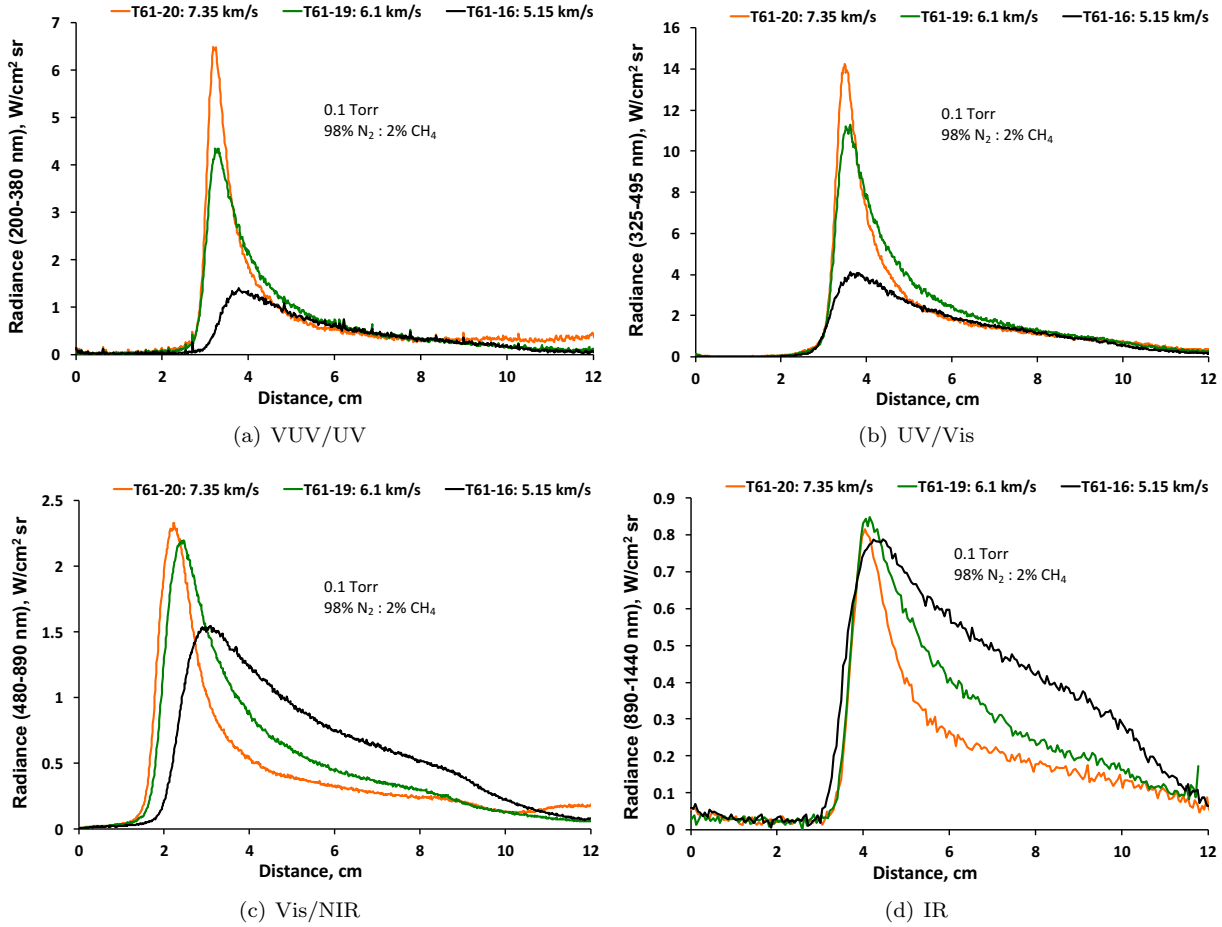

(a) VUV/UV

(b) UV/Vis

(c) Vis/NIR

(d) IR

Figure 15. Radiance measured at 2% CH_4 / 98% N_2 and 0.1 Torr.

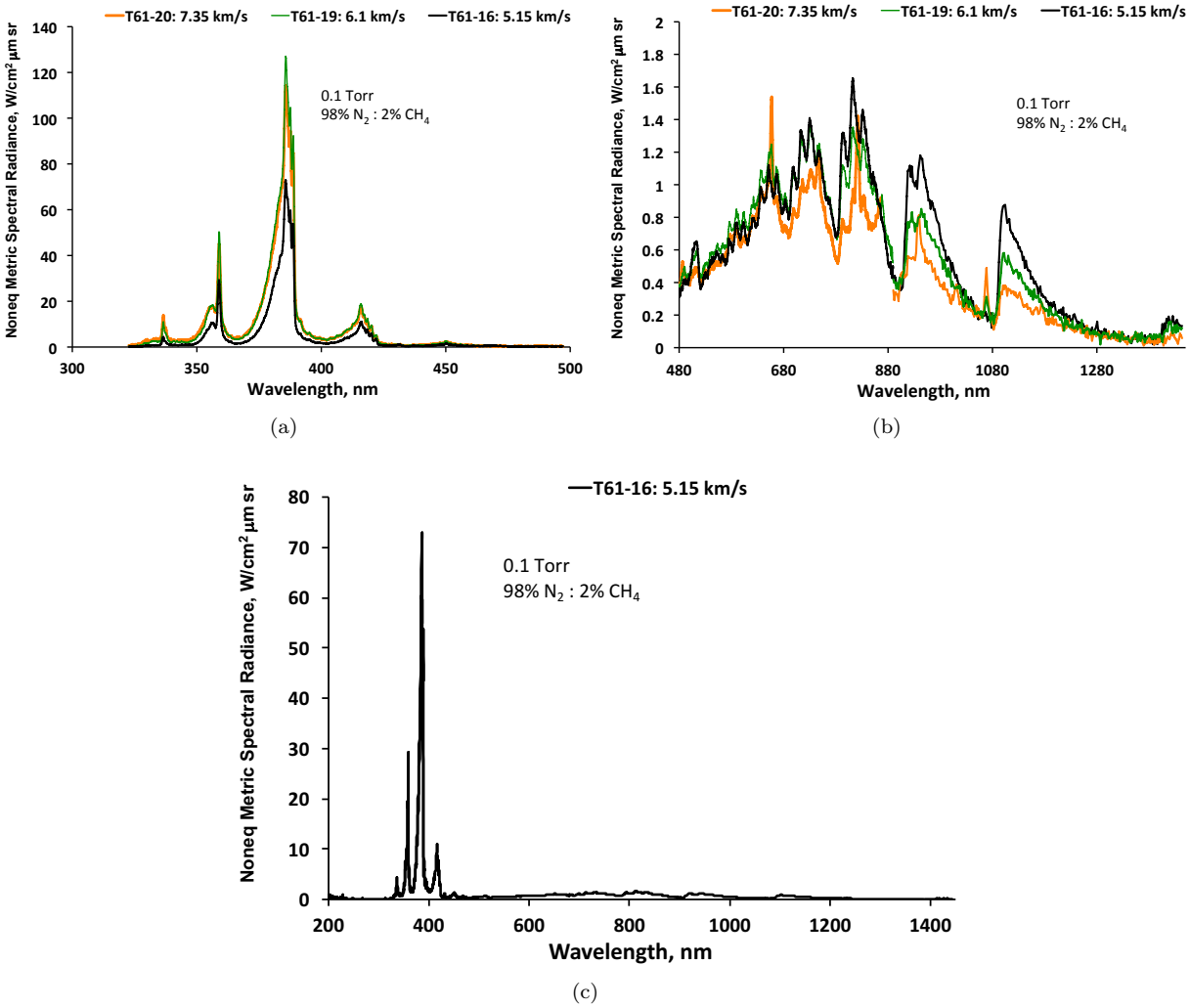

Figure 16. Non-equilibrium metric spectral comparison at 2% CH_4 / 98% N_2 and 0.1 Torr.

VIII. Conclusion

This paper has detailed the data obtained from the recent Titan test campaign conducted in the EAST facility, known as Test 61 and the results are available at https://data.nasa.gov/ [b]. The results have been presented in terms of the peak radiance and non-equilibrium metric as a function of velocity, along with profiles of radiance integrated over wavelength and the non-equilibrium metric applied to spectral radiance. The data from these experiments have been compared to previously reported data from EAST and two campaigns from the X2 facility in Australia. The Test 61 results have been shown to be several factors larger in radiance compared to previous experimental data. In some cases, the discrepancy has been shown to be up to an order of magnitude depending on the metric used. The experiments have also been compared with simulations using DPLR and NEQAIR. Generally, very good agreement has been observed between Test 61 and the simulations over most spectral ranges. In particular, the peak radiance of CN Violet and the decay rate of CN Red were very well matched. However, the magnitude of CN Red and the decay of CN Violet still showed some level of disagreement. Due to the substantial discrepancies observed with previously published shock tube data, a substantial effort was undertaken to ascertain what was the root cause of the differences. In order to achieve this goal, several variations in the operation of the facility were tested. The only option examined that showed improved agreement with the previously published data required contamination to be present in the test gas of the previous campaigns. When air was deliberately added to the test gas in Test 61, based on quoted contamination levels for the X2 facility, the CN Violet radiance dropped by approximately a factor of 2. However, given all the options tried, it was not possible to fully explain all of the discrepancies observed. Finally, experiments showing the best shot characteristics from Test 61 have been selected as sources for future code validation studies and facility-to-facility comparisons. Due to the increased confidence in the Test 61 experiments, it is recommended that the previously reported Titan entry data be replaced with the current data set.

Acknowledgments

The authors would like to thank NASA's Entry Systems Modeling project for their support of this work. Drs Aaron Brandis and Brett Cruden are supported through the NNA15BB15C contract between NASA Ames Research Center and AMA Inc. The authors would also like to acknowledge Mark McGlaughlin, Ramon Martinez, and Rick Ryzinga, for their support in operating the EAST facility.

References

[1]Bose, D., Wright, M. J., Bogdanoff, D. W., Raiche, G. A., and Allen, G. A., "Modeling and Experimental Assessement of CN Radiation Behind a Strong Shock Wave," *Journal of Thermophysics and Heat Transfer*, Vol. 20, No. 2, 2006, pp. 220–230.

[2]Brandis, A., Morgan, R., McIntyre, T., and Jacobs, P., "Nonequilibrium Radiation Intensity Measurements in Simulated Titan Atmospheres," *Journal of Thermophysics and Heat Transfer*, Vol. 24, No. 2, 2009, pp. 291–300.

[3]Jacobs, C., McIntyre, T., Morgan, R., Brandis, A., and Laux, C., "Radiative Heat Transfer Measurements in Low-Density Titan Atmospheres," *Journal of Thermophysics and Heat Transfer*, Vol. 29, No. 4, 2015, pp. 835–844.

[4]Cruden, B., Martinez, R., Grinstead, J., and Olejniczak, J., "Simultaneous Vacuum-Ultraviolet Through Near-IR Absolute Radiation Measurement with Spatiotemporal Resolution in An Electric Arc Shock Tube," *41st AIAA Thermophysics Conference*, San Antonio, Texas, 2009, AIAA-2009-4240.

[5]Joiner, N., Beck, J., Capitelli, M., Fertig, M., Herdrich, G., Laricchiuta, A., Liebhart, H., Lino da Silva, M., Marraffa, L., Nguyen-Bui, N., Reynier, P., and Tran, P., "Validation of Aerothermal Chemistry Models for Re-entry Applications: Theoretical and Computational Synthesis," *Proceedings of the 8th European Symposium on Aerothermodynamics for Space Vehicles*, 2015.

[6]Palmer, G., Prabhu, D., Brandis, A., and McIntyre, T., "Numerical Simulation of Radiation Measurements taken in the X2 Facility for Mars and Titan Gas Mixtures," *42nd AIAA Thermophysics Conference*, Honolulu, 2011. AIAA 2011-3768.

[7]Vargas, J., Lino da Silva, M., and Lopez, B., "Improvement of state-resolved kinetic models applied to N_2 – CH_4 hypersonic entry flows," *7th International Workshop on Radiation of High Temperature Gases in Atmospheric Entry*, Stuttgart, Germany, 2016.

[8]Wright, M., Olejniczak, J., Walpot, L., Raynaud, E., Magin, T., Caillault, L., and Hollis, B. R., "A code calibration study for Huygens entry aeroheating," *44th AIAA Aerospace Sciences Meeting and Exhibit*, Reno, Nevada, 2006, AIAA-2006-382.

[9]Brandis, A., Laux, C., Magin, T., McIntyre, T., and Morgan, R., "Comparison of Titan Entry Radiation Shock-Tube Data with Collisional-Radiative Models," *Journal of Thermophysics and Heat Transfer*, Vol. 28, No. 1, 2014, pp. 32–38.

[10]Cruden, B., "Absolute Radiation Measurements in Earth and Mars Entry Condition," *Radiation and Gas-Surface Interaction Phenomena in High-Speed Re-Entry*, Vol. Von Karman Institute Lecture Series, 2014.

[b]Download EAST data at https://data.nasa.gov/docs/datasets/aerothermodynamics/EAST/index.html

[11]Niemann, H., Atreya, S., Demick, J., Gautier, D., Haberman, J., Harpold, D., Kasprzak, W., Lunine, J., Owen, T., and Raulin, F., "Composition of Titan's lower atmosphere and simple surface volatiles as measured by the Cassini-Huygens probe gas chromatograph mass spectrometer experiment," *Journal of Geophysical Research: Planets*, Vol. 115, No. E12, 2010.

[12]Wright, M., *A Family of Data-Parallel Relaxation Methods for the Navier-Stokes Equations*, Ph.D. thesis, University of Minnesota, 1997.

[13]Wright, M., Candler, G., and Bose, D., "Data-Parallel Line Relaxation Method for the Navier-Stokes Equations," *AIAA Journal*, Vol. 36, No. 9, 1998, pp. 1603–1609.

[14]Wright, M., White, T., and Mangini, N., "Data-Parallel Line Relaxation (DPLR) Code User Manual Acadia-Version 4.01.1," NASA/TM-2009-215388, NASA Ames Research Center, October 2009.

[15]Gökçen, T., "N_2-CH_4-Ar Chemical kinetic model for simulations of atmospheric entry to Titan," *Journal of Thermophysics and Heat Transfer*, Vol. 21, No. 1, 2007, pp. 9–18.

[16]Whiting, E., Park, C., Yen, L., Arnold, J., and Paterson, J., "NEQAIR96, Nonequilibrium and Equilibrium Radiative Transport and Spectra Program: User's Manual," Technical Report NASA RP-1389, Ames Research Center, Moffett Field, Moffett Field, 1996.

[17]Kramida, A., Ralchenko, Y., Reader, J., and Team, N. A., "NIST Atomic Spectra Database, Version 5.0.0," physics.nist.gov/asd/, July 2012, last accessed July, 2012.

[18]Cunto, W., Mendoza, C., Ochsenbein, F., and Zeippen, C., "TOPbase at the CDS," *Astronomy and Astrophysics*, Vol. 275, Aug. 1993, pp. L5–L8, see also http://cdsweb.u-strasbg.fr/topbase/topbase.html.

[19]Tashkun, S. and Perevalov, V., "CDSD-4000: High-Resolution, High-Temperature Carbon Dioxide Spectroscopic Databank," *Journal of Quantitative Spectroscopy and Radiative Transfer*, Vol. 112, No. 9, 2011, pp. 1403–1410.

[20]Laux, C., *Optical diagnostics and radiative emission of air plasmas*, Phd thesis, Stanford University, 1993.

[21]Hyun, S., *SPRADIAN07: Radiation code SPRADIAN07 and its applications*, Ph.D. thesis, KAIST, 2009.

[22]Cruden, B. and Brandis, A., "Updates to the NEQAIR Radiation Solver," St. Andrews, Scotland, November 2014.

[23]Brandis, A., Johnston, C., and Cruden, B., "Non-equilibrium Radiation for Earth Entry," *46th AIAA Thermophysics Conference*, Washington, DC, 2016, AIAA-2016-3690.

[24]Cruden, B. and Brandis, A., "Measurement and Prediction of Radiative Non-equilibrium for Air Shocks Between 7-9 km/s," *47th AIAA Thermophysics Conference*, Denver, CO, 2017.

[25]Brandis, A., Johnston, C., Cruden, B., and Prabhu, D., "Equilibrium Radiative Heating from 9.5 to 15.5 km/s for Earth Atmospheric Entry," Vol. 31, 2017.

[26]Brandis, A., Johnston, C., Cruden, B., Prabhu, D., and Bose, D., "Uncertainty Analysis and Validation of Radiation Measurements for Earth Re-Entry," *Journal of Thermophysics and Heat Transfer*, Vol. 29, No. 2, 2015, pp. 209–221.

[27]Brandis, A., Johnston, C., Cruden, B., and Prabhu, D., "Investigation of Nonequilibrium Radiation for Mars Entry," *51st AIAA Aerospace Sciences Meeting*, Grapevine, Texas, 2013, AIAA-2013-1055.

[28]Brandis, A., Morgan, R., and McIntyre, T., "Analysis of Nonequilibrium CN Radiation Encountered During Titan Atmospheric Entry," *Journal of Thermophysics and Heat Transfer*, Vol. 25, No. 4, 2011, pp. 493–499.

[29]Panesi, M., Jaffe, R., Schwenke, D., and Magin, T., "Rovibrational internal energy transfer and dissociation of $N_2(^1\Sigma_g^+)$ - $N(^4S_u)$ system in hypersonic flows," *The Journal of Chemical Physics*, Vol. 138, 2013.

[30]McBride, B. and Gordon, S., "Computer Program for Calculation of Complex Chemical Equilibrium Compositions and Applications I. Analysis," NASA RP-1311, NASA Glenn, October 1994.

Appendix: Validation Data

The appendix presents the radiance profiles and the non-equilibrium metric spectral radiance for the experiments selected as validation data.

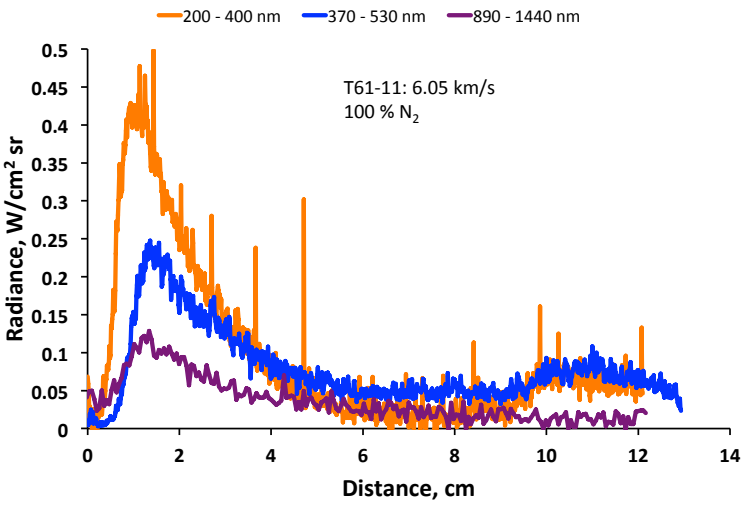

(a)

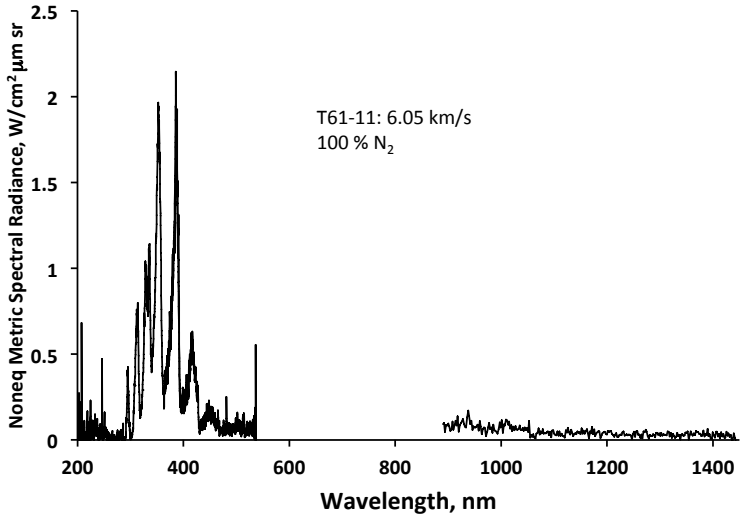

(b)

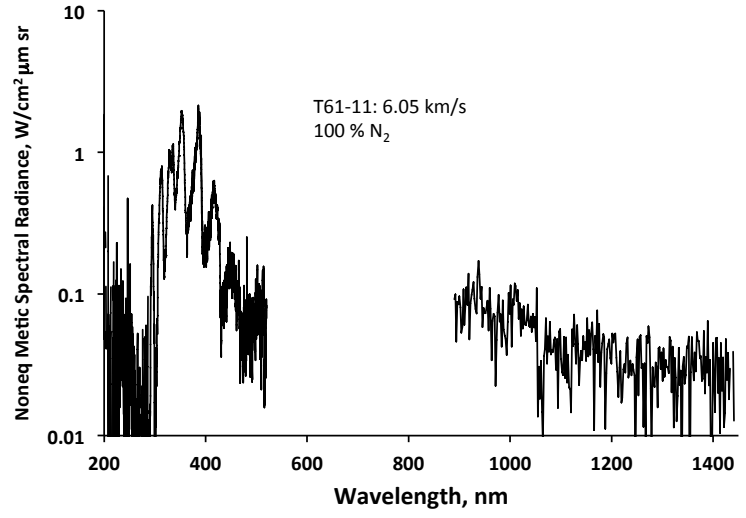

(c)

Figure 17. Benchmark data at 100% N_2 and 0.1 Torr.

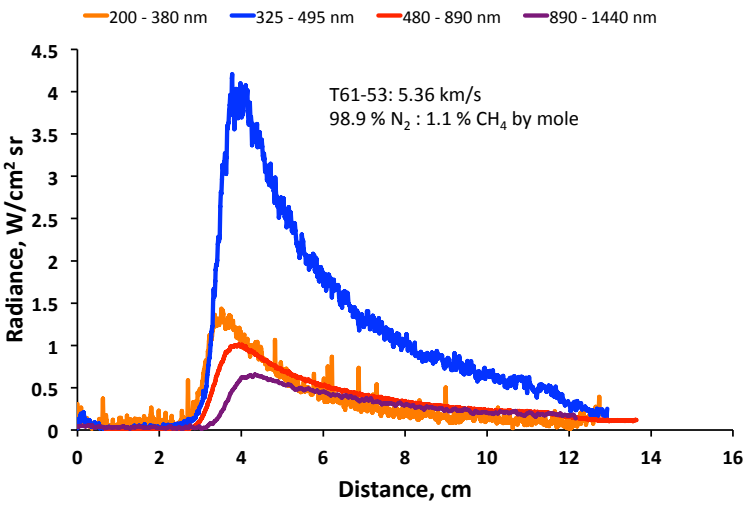

(a)

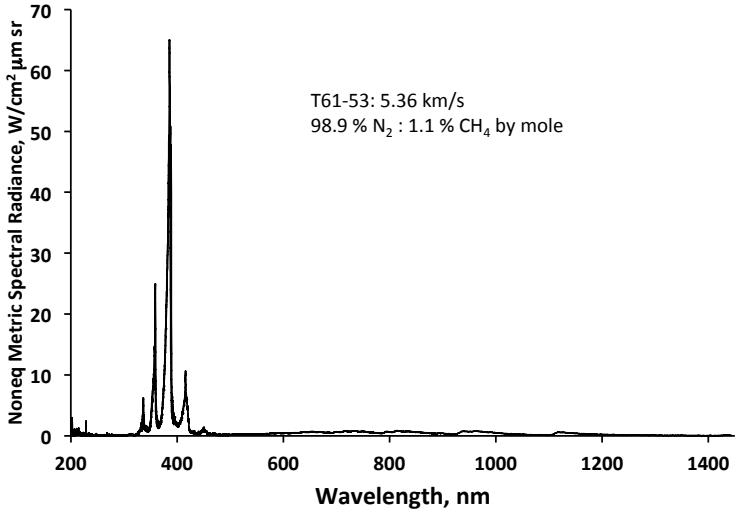

(b)

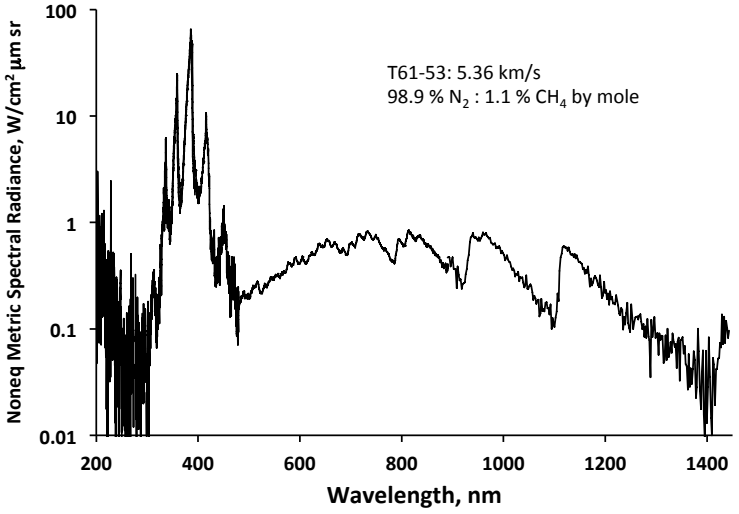

(c)

Figure 18. Benchmark data at 1.1% CH_4 / 98.9% N_2 and 0.1 Torr.

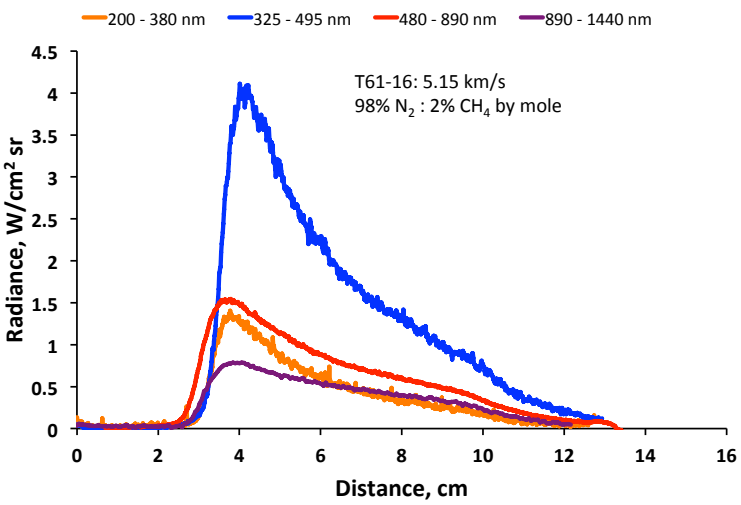

(a)

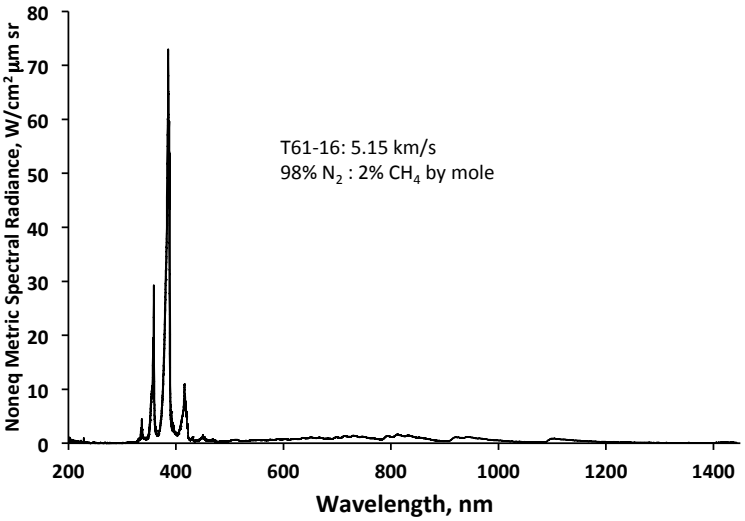

(b)

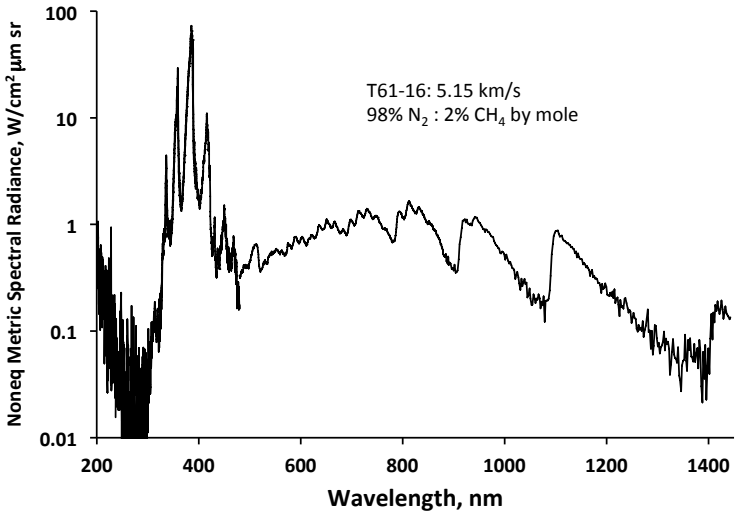

(c)

Figure 19. Benchmark data at 2% CH_4 / 98% N_2 and 0.1 Torr.

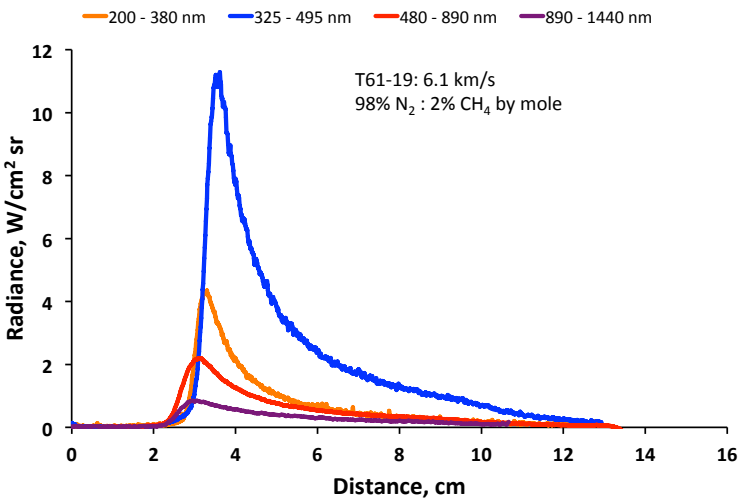

(a)

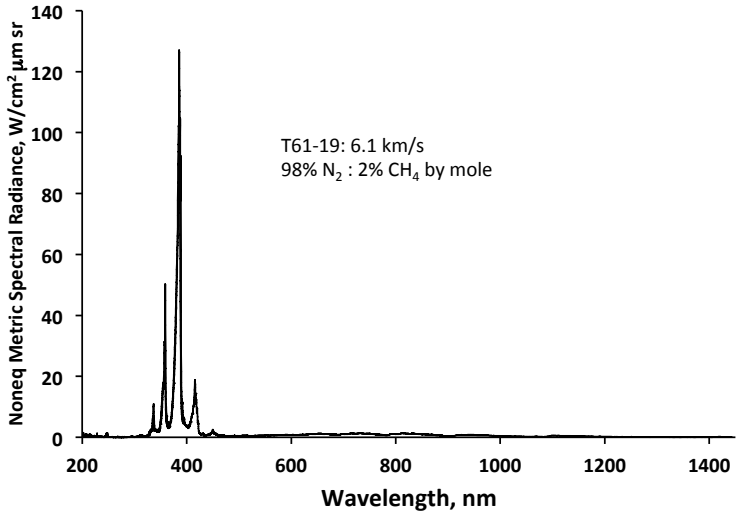

(b)

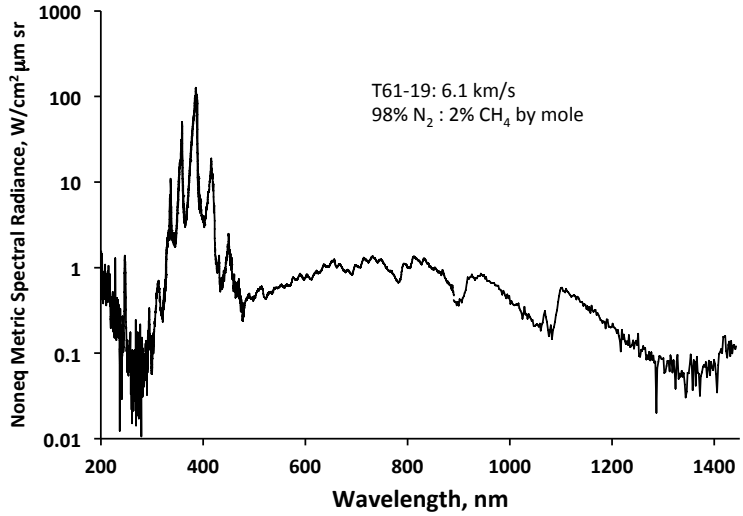

(c)

Figure 20. Benchmark data at 2% CH_4 / 98% N_2 and 0.1 Torr.

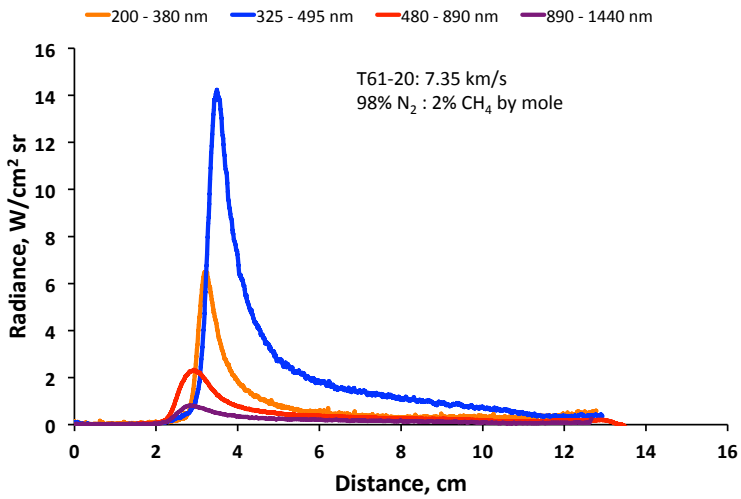

(a)

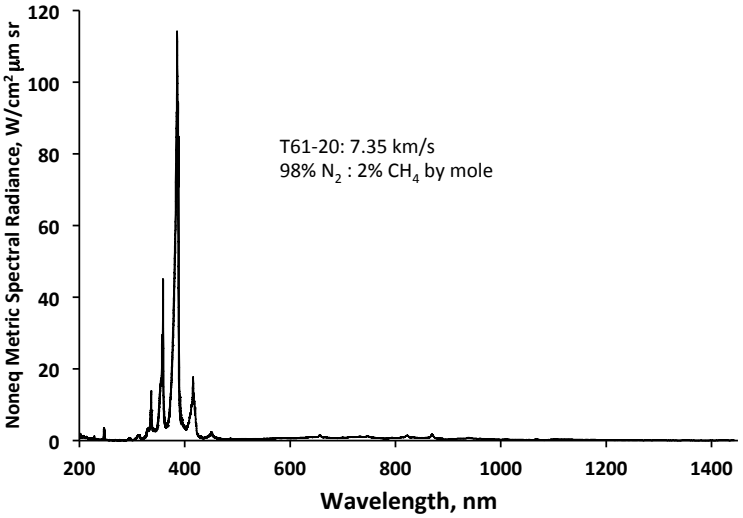

(b)

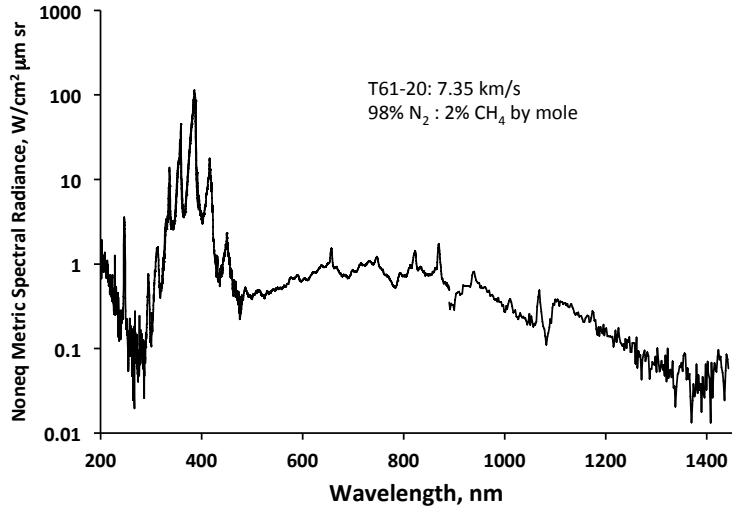

(c)

Figure 21. Benchmark data at 2% CH_4 / 98% N_2 and 0.1 Torr.

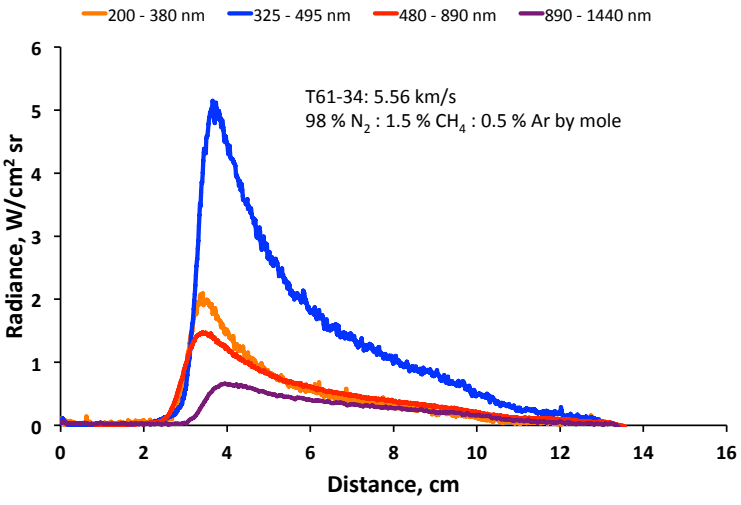

(a)

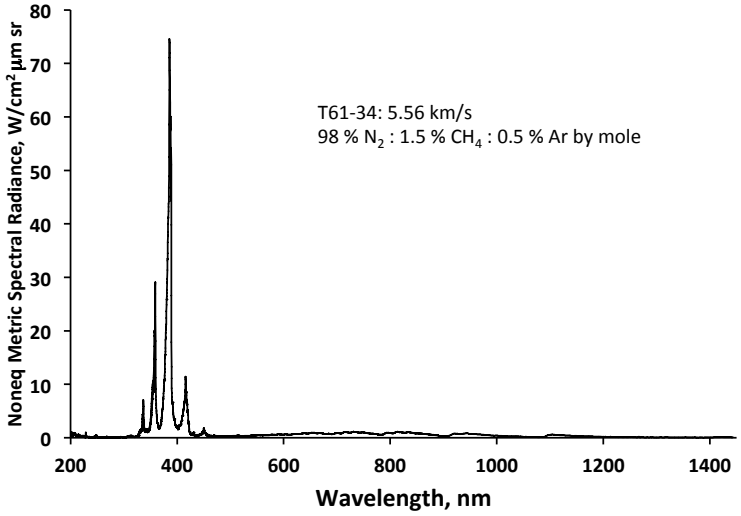

(b)

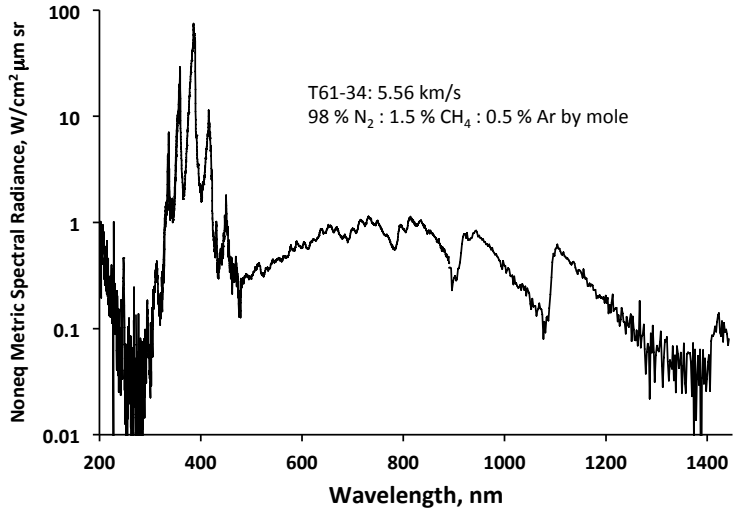

(c)

Figure 22. Benchmark data at 1.5% CH_4 / 98.5% N_2 / 0.5% Ar and 0.1 Torr.

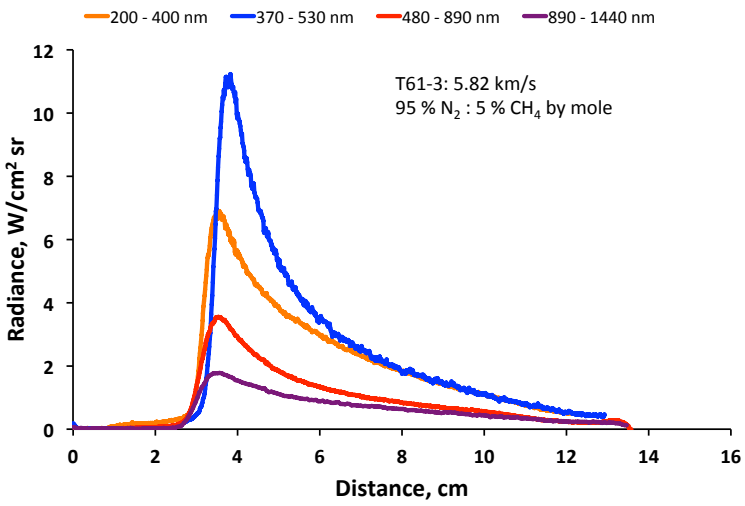

(a)

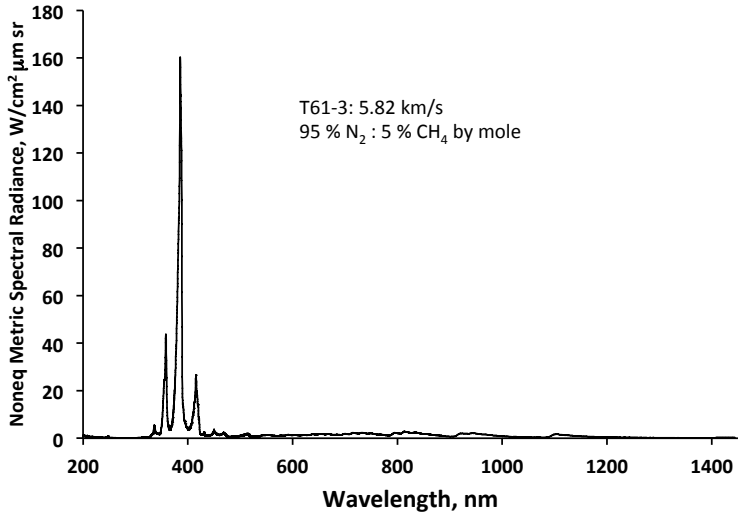

(b)

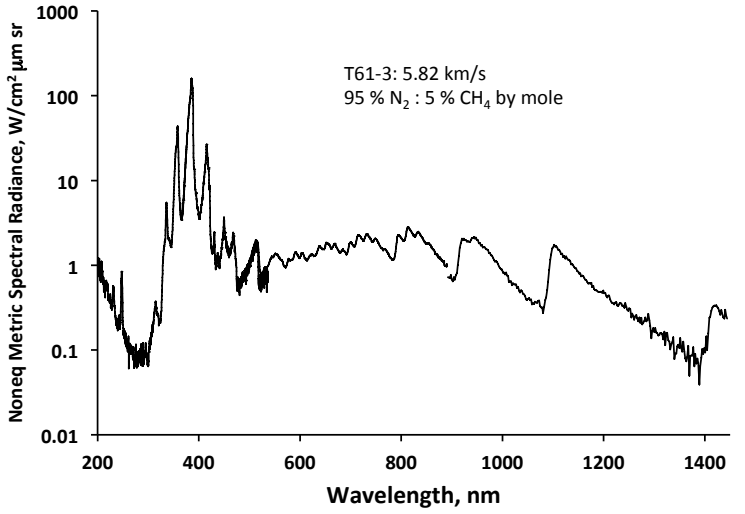

(c)

Figure 23. Benchmark data at 5% CH_4 / 95% N_2 and 0.1 Torr.

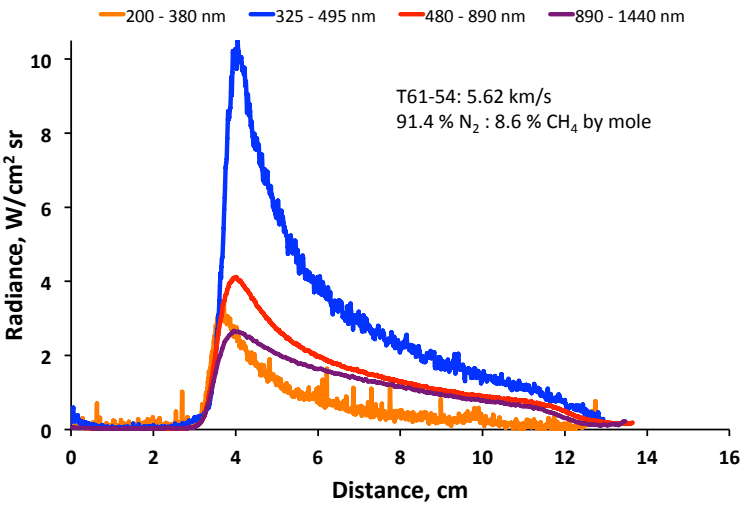

(a)

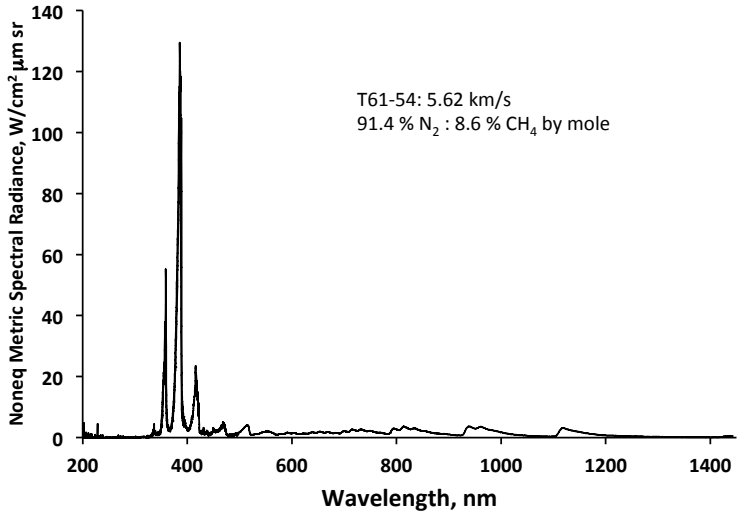

(b)

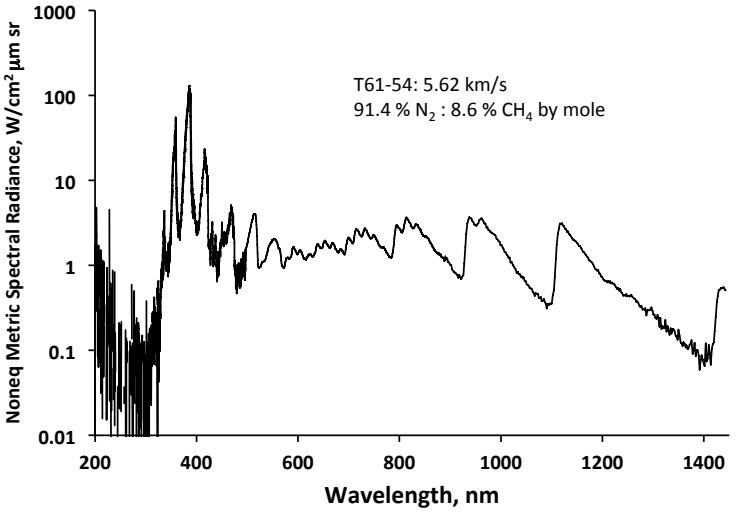

(c)

Figure 24. Benchmark data at 8.6% CH_4 / 91.4% N_2 and 0.1 Torr.